NAVAL POSTGRADUATE SCHOOL

MONTEREY, CALIFORNIA

THESIS

RENEWABLE HYDROGEN PRODUCTION, COMPRESSION, AND STORAGE AUTONOMOUS SYSTEM

by

Benjamin R. Anderson

June 2019

Thesis Advisor: Anthony J. Gannon
Co-Advisor: Andrea D. Holmes

THIS PAGE INTENTIONALLY LEFT BLANK

REPORT DOCUMENTATION PAGE	*Form Approved OMB No. 0704-0188*

1. AGENCY USE ONLY *(Leave blank)*	**2. REPORT DATE** June 2019	**3. REPORT TYPE AND DATES COVERED** Master's thesis

4. TITLE AND SUBTITLE RENEWABLE HYDROGEN PRODUCTION, COMPRESSION, AND STORAGE AUTONOMOUS SYSTEM	**5. FUNDING NUMBERS**
6. AUTHOR(S) Benjamin R. Anderson	
7. PERFORMING ORGANIZATION NAME(S) AND ADDRESS(ES) Naval Postgraduate School Monterey, CA 93943-5000	**8. PERFORMING ORGANIZATION REPORT NUMBER**
9. SPONSORING / MONITORING AGENCY NAME(S) AND ADDRESS(ES) Office of Naval Research, Monterey, CA 93943	**10. SPONSORING / MONITORING AGENCY REPORT NUMBER**

11. SUPPLEMENTARY NOTES The views expressed in this thesis are those of the author and do not reflect the official policy or position of the Department of Defense or the U.S. Government.

12a. DISTRIBUTION / AVAILABILITY STATEMENT Approved for public release. Distribution is unlimited.	**12b. DISTRIBUTION CODE** A

13. ABSTRACT (maximum 200 words)

Implementation of isolated energy production facilities could enhance Department of Defense (DoD) capability in forward-operating bases, ships, vehicles, and even permanent stations. This technology may also benefit the U.S. economy with a new renewable-energy storage alternative. This capability not only reduces dependence on fossil fuels but also reduces environmental impact as combustion products of hydrogen are much cleaner and minimizes CO_2 byproducts. To make this hydrogen generation plant completely isolated with no additional power and operator involvement, there are few steps left in this ongoing Office of Naval Research–funded project.

A major problem facing renewable, sustainable energy sources is the storage issue with current limitations on batteries and supercapacitors. Compressed hydrogen gas presents a potential solution to this problem as hydrogen gas can be stored in tanks for future uses in fuel cells or even gas turbine generators. An entirely autonomous, isolated production and storage system is within grasp at the Naval Postgraduate School. The system in place now has the capability to generate and store compressed hydrogen gas produced through solar power with minimal operator interference.

14. SUBJECT TERMS hydrogen generation, hydrogen compression, hydrogen storage, renewable energy, hydrogen system, solar power, autonomous fuel generation system	**15. NUMBER OF PAGES** 91
	16. PRICE CODE

17. SECURITY CLASSIFICATION OF REPORT	**18. SECURITY CLASSIFICATION OF THIS PAGE**	**19. SECURITY CLASSIFICATION OF ABSTRACT**	**20. LIMITATION OF ABSTRACT**
Unclassified	Unclassified	Unclassified	UU

NSN 7540-01-280-5500 Standard Form 298 (Rev. 2-89)
Prescribed by ANSI Std. 239-18

THIS PAGE INTENTIONALLY LEFT BLANK

Approved for public release. Distribution is unlimited.

RENEWABLE HYDROGEN PRODUCTION, COMPRESSION, AND STORAGE AUTONOMOUS SYSTEM

Benjamin R. Anderson
Ensign, United States Navy
BSME, U.S. Naval Academy, 2018

Submitted in partial fulfillment of the
requirements for the degree of

**MASTER OF SCIENCE IN ENGINEERING SCIENCE
(AEROSPACE ENGINEERING)**

from the

**NAVAL POSTGRADUATE SCHOOL
June 2019**

Approved by: Anthony J. Gannon
Advisor

Andrea D. Holmes
Co-Advisor

Garth V. Hobson
Chair, Department of Mechanical and Aerospace Engineering

THIS PAGE INTENTIONALLY LEFT BLANK

ABSTRACT

Implementation of isolated energy production facilities could enhance Department of Defense (DoD) capability in forward-operating bases, ships, vehicles, and even permanent stations. This technology may also benefit the U.S. economy with a new renewable-energy storage alternative. This capability not only reduces dependence on fossil fuels but also reduces environmental impact as combustion products of hydrogen are much cleaner and minimizes CO_2 byproducts. To make this hydrogen generation plant completely isolated with no additional power and operator involvement, there are few steps left in this ongoing Office of Naval Research–funded project.

A major problem facing renewable, sustainable energy sources is the storage issue with current limitations on batteries and supercapacitors. Compressed hydrogen gas presents a potential solution to this problem as hydrogen gas can be stored in tanks for future uses in fuel cells or even gas turbine generators. An entirely autonomous, isolated production and storage system is within grasp at the Naval Postgraduate School. The system in place now has the capability to generate and store compressed hydrogen gas produced through solar power with minimal operator interference.

THIS PAGE INTENTIONALLY LEFT BLANK

TABLE OF CONTENTS

LIST OF FIGURES

LIST OF TABLES

THIS PAGE INTENTIONALLY LEFT BLANK

LIST OF ACRONYMS AND ABBREVIATIONS

ACRONYMS

AC	alternating current
ASME	American Society of Mechanical Engineers
CCW	Connected Components Workbench
CFR	United States Code of Federal Regulations
CGA	Compressed Gas Association
CO_2	carbon dioxide gas
DC	direct current
DoD	Department of Defense
DOE	Department of Energy
EHC	electrochemical hydrogen compressor
ESTEP	Energy Systems Technology Evaluation Program
FOB	forward operating bases
H_2	hydrogen gas
N_2	nitrogen gas
NASA	National Aeronautics and Space Administration
NFPA	National Fire Protection Association
NPS	Naval Postgraduate School
ONR	Office of Naval Research
PC	personal computer
PEM	proton exchange membrane
PID	proportional integral derivative
PLC	programmable logic controller
PSIG	pounds per square inch gauge
PV	photovoltaic
SSR	solid state relay
UAV	unmanned aerial vehicle
USB	universal serial bus
UUV	underwater unmanned vehicle

SYMBOLS	**Units**
A	amps
C	coulombs
GW	gigawatt
inHg	inches mercury
J	joules
kg	kilogram
km	kilometer
kWh	kilowatt-hours
L	liters
mA	milliamps
mol	moles
mV	millivolts
P	pressure
P	power
PJ	petajoule
slpm	standard liters per minute
V	volts

ACKNOWLEDGMENTS

First I would like to thank my wife for supporting me through this accelerated program at NPS. I could not have finished my part of this thesis without her. I also want to thank my advisors, Dr. Gannon and Andrea Holmes, for their support with this thesis. Thank you for helping me get up to speed since there were no students working on it when I arrived. I want to thank John Gibson for supporting my work by providing supplies and machining. Jonathon Alvarado has also been instrumental in the completion of the coding for the production facility and making it possible to complete my thesis. Last, my sincere gratitude to Dr. Hobson and CDR Crane for their support and interest in me and the other Shoemaker scholars for the inaugural year of this 609 Shoemaker Scholar program. This extraordinary effort would not be possible without the sponsorship of the Office of Naval Research (ONR) Engineering Systems Technology Evaluation Program (ESTEP) and technical monitoring of Marissa Brand.

THIS PAGE INTENTIONALLY LEFT BLANK

I. INTRODUCTION

As an ongoing Naval Postgraduate School (NPS) project, this research furthers the development of a renewable-powered, hydrogen gas compression and storage station. The specific task of this research is to automate a new, electrochemical hydrogen compressor (EHC) and storage station and connect it to an existing hydrogen production system. Funded by the Office of Naval Research (ONR) Engineering Systems Technology Evaluation Program (ESTEP), the purpose of this renewable energy system is to develop a hydrogen production and storage facility that could be implemented in shore installations, forward operating bases, and possibly even at sea.

A. MOTIVATION

Within the federal government, the Department of Defense (DoD) consumes 78 percent of the total government energy consumption, according to the U.S. Energy Information Administration, and is looking to increase its use of renewable energy. Although DoD energy use has been falling in recent years to 791 PJ (0.75 quadrillion Btu), there is a potential security threat because of dependence on foreign energy sources consisting mostly of crude oil and liquid fuels [1]. There are two categories of energy consumption within the DoD: installation and operational energy consumption. Operational energy makes 70 percent of the total energy needs and consists of "transporting, training, and sustaining personnel and weapons specifically for military operations," while the installation energy includes powering military installations and vehicles not used on combat missions [1]. Of the DoD's 300,000 buildings across more than 500 installations, the Navy and Marine Corps uses 28 percent of the installation energy and 32 percent of the operational energy consumption. Rather than transporting fuel across the world to bases, the DoD would rather shift to energy production capabilities that deploy or generate in the area of operation [1].

The Secretary of the Navy in the *Strategy for Renewable Energy* in 2012, set to accomplish the goal of obtaining at least half of the shore-based energy requirements from renewable energy sources, including solar, wind, and geothermal. This program, as part of the 1 GW initiative for shore-based power generation, projects the current goal to be met by 2020.

As of 2012, 18.6 percent of shore-based energy comes from renewable sources [2]. The Navy met its goal ahead of schedule largely because of the 210 MW solar facility in Arizona and other contracted projects completed before 2017. Having independent sources of power greatly decreases the vulnerability of U.S. bases if physical attackers, cyber attackers, or even natural disasters shut down the public grid [3]. There are other reasons for the dramatic investment in renewable sources, including reduction of energy imports and environmental impact. As stated by the former secretary of the Navy, the Honorable Ray Maybus in the *Strategy for Renewable Energy*, focus on the "unprecedented capacity for continuity of operations when the regional grid becomes unstable … alleviating increasing grid congestion and consumer demand" in accordance to national energy goals [2].

Although hydrogen as a fuel does not fit into the current renewable energy strategy, beyond 2020 there will be increased demand for renewable sources, and hydrogen has the potential to fulfill a vital role in the renewable energy mission of the DoD and the U.S. Navy. Renewably sourced energy is not always needed at the time that it is produced and hydrogen is a useful energy medium that can also dramatically reduce pollution output. Although hydrogen is the most abundant element in the universe, hydrogen requires energy to be collected in a useful form. Currently, 95 percent of hydrogen is produced from either wood or fossil fuels in a process called natural gas reforming according to the Department of Energy's (DOE) Office of Energy Efficiency and Renewable Energy [4]. These methods have byproducts of carbon dioxide (CO_2) along with other pollutant gasses. The hydrogen made from these methods is not considered "green" because of the byproducts associated. A significantly cleaner method to produce hydrogen is electrolysis of water powered by a renewable source, but only about four percent is produced via electrolysis as of 2015 [4].

Hydrogen produced using electrolysis (hydrolysis) requires a large amount of energy to split water into its constituents of hydrogen and oxygen gases at atmospheric pressure. In Dincer's paper, "Green Methods for Hydrogen Production," green hydrogen production is defined as hydrogen that comes from a renewable source. Dincer notes that hydrolysis using off-the-shelf components for hydrolysis can be both inefficient and costly, but has potential as a commercially available system. With improved efficiencies, it will continue to become more viable [5]. Compared to gasoline, diesel, and other liquid fuels, hydrogen, since it has a

very low energy density at atmospheric pressure, has a significantly lower volumetric density, but more than double the gravimetric density. Furthermore, with current limitations on batteries and super capacitors, at high pressure, hydrogen can outperform on the volumetric basis for storing electrical energy [6]. Hydrogen gas has been proven as an attractive alternative fuel that burns significantly cleaner than hydrocarbon products. It can also be used in fuel cells that are pollution free with only water as the byproduct [7].

Active research of hydrogen gas turbines and fuel cells is ongoing at NPS. Combustion of hydrogen in turbines is difficult, primarily due to its high flame temperature and laminar burning velocity causing flashback and subsequent damage to the turbine [8]. Concurrent work at NPS is adapting the Capstone Microturbine Model C30 to run on hydrogen gas instead of natural gas [8]. According to the DOE, fuel cells have been used successfully in notable cases including NASA space shuttles, prototype cars, and other small portable devices, but fuel cells have not been widely implemented because of cost, performance, and durability. The DOE notes that the lack of hydrogen fuel cells is mostly due to the prevalence of cheaper conventional fuels and matured battery technology. At this time, hydrogen is not cost effective to compete with gasolines prices. Plus, the efficiency of hydrogen production, which includes equipment, operations, and maintenance remains the greatest challenge for full scale implementation of hydrogen [4] [6]. However, the development of hydrogen technologies and improved system efficiencies are critical to reducing the demand for conventional fuels to pursue a significantly cleaner alternative. As regulation or availability will lead to the replacement of conventional energy, many policy makers and researchers predict hydrogen will be a premier fuel alternative in what has been hailed as the “Hydrogen Economy” [9].

B. OBJECTIVES

The objective of this research is to further the design of the NPS hydrogen production and storage facility as a proof of concept system. From the previous work of Aviles [10] and Yu [11], the system utilizes solar photovoltaic (PV) electricity to extract water from ambient air splitting water into hydrogen and oxygen using electrolysis also demonstrating a 100 W fuel cell. Birkemeier [12] implemented control and automation of the production system.

Fosson [13] developed the storage facility and evaluated different ranges of hydrogen electrochemical (EHC) compressors and mechanical compressors. The next step was to combine the generation and storage system with a new EHC and demonstrate the ability to autonomously store renewably sourced hydrogen at high pressure. The hydrogen must exhibit acceptable levels of purity through proper purging procedures before use and filtration of contaminants and moisture before entering storage tanks. This work combines the elements of renewable production and efficient energy storage. Continuing work will be focused on the complete automation of the entire system and isolation from grid power.

Accomplishing these objectives will help pave the way for future work of increasing the overall efficiency of the NPS system as a competitive renewable energy storage system. In the future, it can be scaled and modified to become a portable and scalable autonomous energy production and storage system that will increase DoD capabilities and range of operations around the world. This system can also aid in reaching the DoD renewable energy production goals by ensuring that excess renewable energy is stored in a useful medium as high-pressure hydrogen gas for future use. This type of system will provide sustainable energy storage solutions for shore installations where renewable energy is already implemented. Additionally, it can be used for the power requirements of forward operating bases (FOB) and mobile hospitals. Another benefactor could be the Navy's future fleet of aerial unmanned vehicles (UAV) and underwater unmanned vehicles (UUV), which already serve mission critical roles in combat. A deployed fuel production facility in the size of a standard shipping container could sustain drone operations and FOB power requirements. This energy independent system will potentially extend operational range while decreasing logistical support.

C. HYDROGEN PRODUCTION SYSTEM IMPLEMENTATION

1. Storage Method

The hydrogen economy is a novel idea stemming from John Bockris's talk at General Motors Technical Center in 1970 [14]. Hydrogen is very attractive due to its cleaner combustion compared to conventional fuels while it also has a very high energy density per mass [14]. However, at atmospheric conditions, its energy density per volume is extremely

low and thus requires a densification method to store any useful amount of energy. Options for storing hydrogen can be summarized into physical-based and material-based methods as shown in Figure 1, according to the DOE. The most straightforward method to store hydrogen is in a compressed gas form. Compressed gas does not require extraction or extra treatment once stored. Comparatively, liquid hydrogen requires cryogenic temperature conditions because it will boil at atmospheric pressure at - 258°C (- 423°F). Cold/cryogenic compressed hydrogen, another physical-based form, is also difficult because it requires additional energy to maintain the extreme cold temperatures and pressures making it less cost effective for storage. In addition, the material-based hydrogen technologies are still an active area of research requiring additional treatments to be made usable once stored [6].

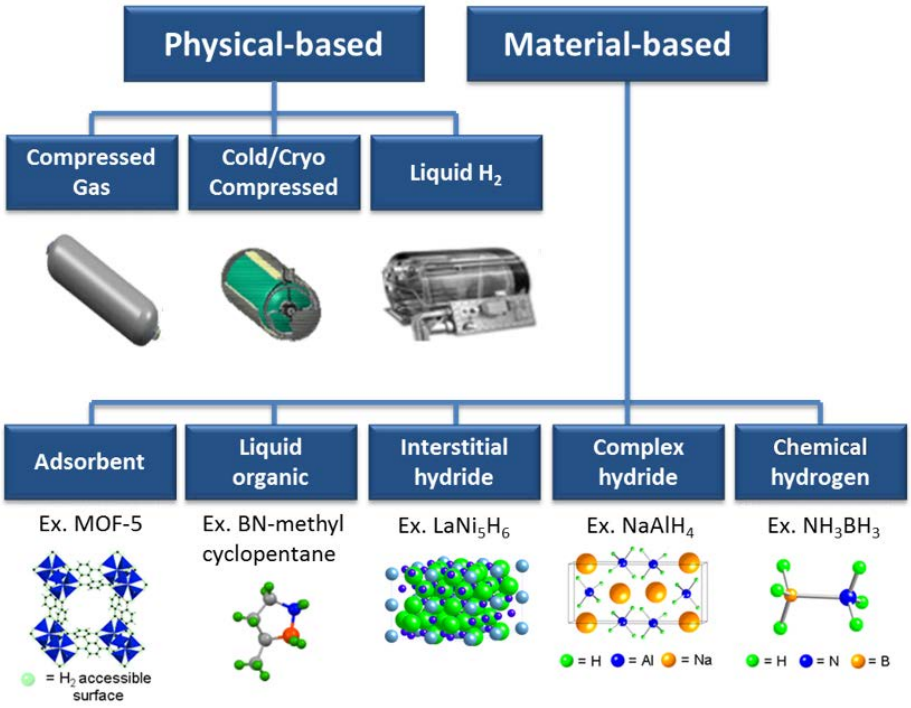

Figure 1. Types of Storage Methods. Source: [4].

In Sarkar and Banerjee's analysis on hydrogen storage options, they concluded that hydrogen gas "seems to be the most favorable for long term viability" and "the total energy required for compressed gas option is the lowest" [15]. Compressing hydrogen (at 345 bar

or about 5000 psi) greatly increases its energy density per volume, making it a good option for immediate use in fuel cells or turbines simply requiring a pressure regulator to convert the high pressure hydrogen to the working inlet pressure. Sarkar and Banerjee performed an energy comparison of the mainstream storage techniques to store hydrogen. Table 1 shows a summary of the results of Sarkar and Banerjee's results for the energy required for producing 1 kg of hydrogen and transporting 1 km.

Table 1. Energy Comparison of Proven Storage Options for Hydrogen. Adapted from [15].

	Compressed Gas Tank	Cryogenic Compressed Tank	FeTi Hydride Sorbent	Mg Hydride Sorbent
Direct energy Required to Travel (kJ)	749 (base)	768	965.4	1164
Energy required to produce and store (kJ)	1260.7	2172.7	1473.7	1777
Energy required to produce tank (kJ)	34.2	15.6	177.3	60
Total energy required (kJ)	2043.9	2956.3	2616.4	3001.5

According to Stetson in the DOE's evaluation of Hydrogen Storage Program Overview, the projected goal cost of hydrogen per kilogram should be $333 by 2020, and currently 700 bar (10,000 psi) compressed hydrogen costs $500 per kilogram. Its gravimetric density and volumetric density of 1.4 kWh/kg and 0.8 kWh/L, respectively, means that at this pressure, hydrogen is very competitive with any other current storage capability. However, at $15 per kWh, the ultimate DOE target of $8 per kWh will require improved methods of production in the future. The other leading sorbents, iron-titanium hydride and magnesium hydride are similar on a price comparison scale, but compressed hydrogen is still the most

attractive storage option when considering the additional processes necessary to extract hydrogen from a sorbent to become usable [16].

2. Compression Method

Since compressed gas is the desirable storage mode, compression of hydrogen is done primarily in two methods: mechanical compressors or solid-state electrochemical hydrogen compressors (EHC). Research and comparison completed at NPS by Fosson [13] concluded that EHCs are better suited for this application, but EHCs may be prone to developing leaks and have not yet been reliable for long term use at the Naval Postgraduate School's hydrogen compression system. EHCs follow an isothermal compression process while mechanical compressors follow adiabatic compression processes. Significantly less energy is required for EHCs compared to hydrogen mechanical compressors to achieve the same pressure ratio in a single stage [13]. Additionally, EHCs have no moving parts, no frictional losses, and few heat losses. Another major advantage is hydrogen is purified with the reaction through the EHC's membrane with no additional hazardous chemicals required [13]. Because the hydrogen is humidified, the water should be removed before storage to avoid corrosion.

Figure 2 shows the basic process of how low-pressure hydrogen oxidizes on the anode. The proton exchange membrane carries the split hydrogen proton across the membrane to reform with the electron at the cathode in its reduction reaction. Over time, the amount of reformation reactions will cause the pressure to increase as more hydrogen reforms on the opposite side of the membrane. A DC power supply is required across the membrane to facilitate the reaction. The oxidation and reduction reactions are as follows: $H_2 \rightarrow 2H^+ + 2e^-$ and $2H^+ + 2e^- \rightarrow H_2$ respectively.

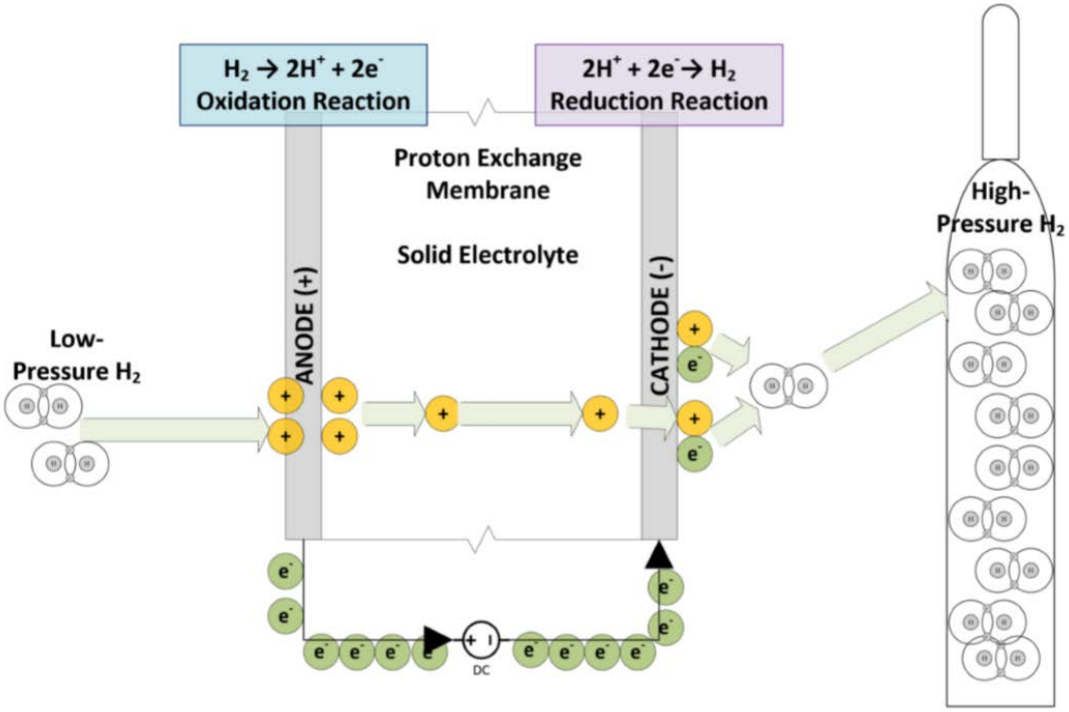

Figure 2. Electrochemical Hydrogen Compression Diagram. Source: [13].

EHCs are able to achieve much higher compression ratios than mechanical compressors. They also have the potential to last much longer than mechanical compressors, which have a mean time before failure of 900 hrs according to results published by the National Renewable Energy Lab [17]. Since there is no need for integrated cooling or lubrication, there are limited maintenance requirements. Lipp's research has shown EHCs can perform without reduction in performance in excess of 10,000 hrs [18]. Mechanical compressors will require oil lubrication and cooling fluid that will inevitably contaminate the hydrogen. Mechanical hydrogen compressors also typically have higher flow rates and will not start and stop as easily as an EHC [13].

The main problem with EHCs deals with their vulnerability to internal leaks in the membrane and degradation of the membrane when in contact with contaminants. EHC reliability has not been widely established prior to this research at NPS in Fosson's research [13], and the development of EHC at has not matured in comparison to the other commercially available subsystems. However, like any new technology, these devices will

continue to improve with advancements mainly in the proton exchange membrane for efficiency and higher outlet pressures. Currently, there are only a few options for commercially available EHC manufacturers including HyET, Xergy, Nuvera, and Sintef.

3. Hydrogen Production Method

There are a few different ways that hydrogen can be produced. According to DOE estimates, 95 percent of hydrogen is produced from either wood or fossil fuels in natural gas reformation. These methods do not contribute to an energy independent model because they require non-renewable fuels. Hydrogen produced using electrolysis requires a large amount of energy to separate water into hydrogen and oxygen gasses. This method produces relatively pure hydrogen gas. If electrolysis is accomplished by renewable energy technology, it can be an effective and clean method of hydrogen production that increases energy resilience [4]. In order to maintain production of high-quality hydrogen, electrolysis is the clear choice for implementation on an isolated, renewable energy production system.

Electrolysis by means of an electrolyzer consists of an anode and cathode in an electrolytic cell that operates using DC voltage and current. The reaction must be facilitated using an alkaline electrolyte within the solution, a polymer electrolyte membrane, or a solid ceramic material [5]. Adding an electrolyte to distilled water is the simplest way to facilitate the splitting reaction shown in Figure 3. This is where hydrogen and oxygen atoms split and reform at the anode and cathode, respectively, as gas bubbles. The proton exchange membrane with an electrolytic solution works similarly with higher efficiencies, but the device is very sensitive to the water purity. Solid electrolyzers are another possible way to facilitate the disassociation reaction but require a larger power input to achieve temperatures between 700–800°C (371-427°F). This is not practical for a renewably powered system with limited power [4].

Figure 3 shows the diagram of an electrolyzer that utilizes an electrolyte and membrane to separate the anodic and cathodic reaction region to collect the byproduct gasses of hydrogen and oxygen. The power supply promotes hydrogen and oxygen breaking its molecular form to form oxygen at the anode and hydrogen at the cathode. The hydrogen protons move through the electrolyte solution and membrane to reform as

hydrogen gas at the cathode. The electrolyte solution contains hydroxide ions (OH^-) usually supplied by potassium hydroxide (KOH) solution or another electrolyte in distilled water [4]. A concentration of 20 to 30 percent is required for operation. Electrolyzers of this type are typically very reliable and capable of achieving up to 99.99 percent pure hydrogen [5]. Coupled with a renewable energy source, this makes hydrogen produced via electrolysis a worthwhile investment for the fuel of the future. Such devices are between 50 and 65 percent efficient [5].

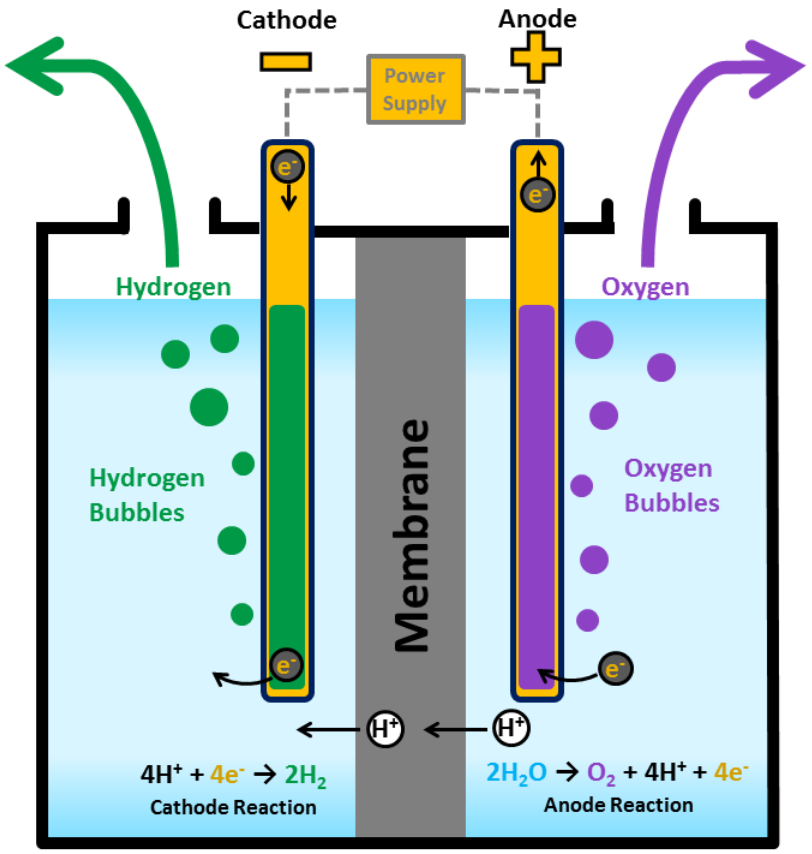

Figure 3. Electrolyzer Diagram. Source: [4].

4. Water Production

For a self-sufficient plant, water collection is a necessity for electrolysis. There are a few ways to harvest distilled water from natural sources. The first method is by dehumidification. Dehumidification involves a refrigeration cycle that reduces the air's

ability to hold moisture. The air passes through cold coils where moisture in the air condenses and is collected in the reservoir. Another option for sourcing distilled water is solar distillation, which would require a water source and area for panels. Solar energy transmits through a clear material. This causes water to evaporate onto a cover material. The water is then collected in a reservoir. Solar distillation may be more suitable where water is already available, but dehumidification has wider applicability for an isolated FOB. Humidity levels will vary from place to place, but at NPS in Monterey, CA the average relative humidity is 75% [19]. Dehumidification technology has been proven effective even in climates with humidity as low as 40 percent. Research by Kim has shown that even at 10 percent relative humidity, a maximum of 0.25 liters of water per kilogram of air can be produced [20].

5. Renewable Energy Source

There are many options available for renewable energy today, but few have as much versatility for location and maturation as solar energy. Photovoltaic (PV) systems are primarily used for electrical power and are only 15 percent efficient on average. However, new innovations in material science have enabled at least five mainstream manufacturers to break the 20 percent threshold with some researchers attaining even higher results [21]. Solar energy is the third most common renewable energy power source behind hydropower dams and wind turbines. In cases where power demand is low and the supply of grid-tied solar power is high such as the middle of the day, the excess solar power can flood the grid causing potential blackouts or be underutilized. In California, where solar energy has quickly risen from 0.5 to 10 percent of its renewable energy from 2010 to 2016, the neighboring state of Arizona was paid to take the excess production to avoid blackout by over-flooding the grid [22]. As PV power continues to expand as a viable option for renewable power generation, there will be significant challenges to restructuring the grid for storage capability and stability to avoid solar overload.

The answer to the excess solar energy is obviously storage, and the answer will come from a combination of energy storage solutions that will feature batteries, super-capacitors, and hydrogen fuel. Batteries are a mature energy storage technology compared

to the others and have sufficient capability for most applications. One area that showcases the energy density advantages of stored hydrogen is hydrogen cars over battery-powered electric vehicles. Thomas has shown that "for any vehicle range greater than 160 km (100 miles) fuel cells are superior to batteries in terms of mass, volume, cost, initial greenhouse gas reductions, refueling time and … energy efficiency" [23]. Supercapacitors can also be used for storing electrical energy and can be cycled at faster rates compared to lithium-ion batteries. Nevertheless, they are still in the developmental phase with similar energy density issues as batteries [24]. For expanded DoD capability, the use of an energy dense medium is critical for storing energy in a FOB or remote outposts with limited payload capabilities.

D. IMPLEMENTATION OF HYDROGEN SYSTEMS

The first wind-powered hydrogen micro-economy was built on the small remote Norwegian island of Utsira in 2004. In a pilot project by Norsk Hydro and Enercon, wind turbines powered a miniature, autonomous hydrogen economy [25]. When excess wind power was generated on the power grid, electrolyzers produced hydrogen. Ulleberg notes in his summary journal article of the project that hydrogen generation was particularly needed when consumer demand was low and power generation was high in order to help stabilize their power grid. When wind power was not utilized, a 10 kW hydrogen fuel cell and 55 kW hydrogen engine met the real energy demands of the 10 households tested within the pilot project. At 200 bar (2900 psi) storage capability and with no wind power, the system could provide customers energy for up to three days. However, the main problems with the system during its four-year test cycle focused on longevity and inefficiencies of the electrolyzer, fuel cell, and hydrogen engine, which contributed to an overall system efficiency of only 20 percent of the wind energy utilization [25]. Ulleberg also notes other demonstration plants that have accomplished similar systems with alternative sources in the U.S., Argentina, Greece, and the United Kingdom [25].

The question remaining is, how can hydrogen energy be scaled to meet future energy needs of transportation which primarily consumes non-renewable fuels? In Ball and Weeda's paper, "The Hydrogen Economy – Vision or Reality?" the scalability is evaluated

based on current development initiatives. About 16,000 km of hydrogen pipelines exist in Europe, Asia, and the U.S. However, only 300 hydrogen refueling stations exist compared to 400,000 conventional refueling stations globally. Although in its infancy, the development of prototype stations and standardized pressures at 350 bar for buses and equipment and at 700 bar for automobiles will lead to an expedited infrastructure starting with metropolitan areas as networks gradually expand. However, the authors note that development initiatives by the government are the key to incentivizing both consumers and manufacturers to convert to fuel cell vehicles. The development of green hydrogen through hydrolysis must also be scaled through government incentives to develop a low-cost infrastructure that can compete against non-renewable hydrogen production. This will eventually require a more extensive pipeline to connect with a growing refueling station network [26].

The DoD has already made significant investments using hydrogen. Hickam Air Force Base and Marine Corps Base in Hawaii, in conjunction with the State of Hawaii, have functional hydrogen fuel station projects that utilize PV arrays. These projects show a potential energy independent model for isolated installations with hydrogen-fueled government vehicles [27]. General Motors is currently working on projects for the Navy to create a hydrogen powered UUV that will increase the capability and awareness of submarines and surface ships [28]. The U.S. Naval Research Laboratory has awarded a contract for further development of the Hybrid Tiger UAV as a flexible solar cell and hydrogen fuel cell powered drone for long range missions. It has already demonstrated flight times of over 26 hours with a compressed hydrogen tank [29]. These projects are certainly only the beginning of hydrogen capabilities in the DoD. Hydrogen fuel will continue to be an integral part of powering installations and military operations.

THIS PAGE INTENTIONALLY LEFT BLANK

II. DESIGN STRATEGY AND SAFETY

For combining an autonomous renewable hydrogen production plant with an existing storage facility, a variety of EHC compressors were used for testing and evaluation. An operator is required for start-up to execute the purge cycle, but the system has capabilities to shut down without user interference if desired. Modifications were made to the existing systems in order to accomplish compression and storage of renewably sourced hydrogen which has not been demonstrated previously. The existing storage system is rated up to 206 bar (3000 psi) and maintains adherence to the safety regulations specified through by the Compressed Gas Association's (CGA) guidelines for Hydrogen storage [30] which references National Fire Protection Association [31], International Codes, International Fire Code, International Fuel Gas Code, end user piping systems regulations [32], and American Society of Mechanical Engineers (ASME) standards for piping and pressure vessels [33].

This research focuses on giving insight into the remaining processes that require automation in the system. There are two primary means of controlling hydrogen purity being stored in the storage tanks. The first method utilizes purge cycles to reduce the concentration of other gasses within the system. The second utilizes high pressure filters to reduce moisture content and possible particulates from entering the pressure vessels. The system must have measurements and data capture ability for characterization and further optimization or component upgrades. Safety measures of passive and active autonomous controls were implemented to the compressor and storage station. A demonstration of system must first be accomplished before system can be completely independent and autonomous.

A. CHARACTERISTICS OF GASEOUS HYDROGEN

Hydrogen is a colorless, odorless, non-toxic, and flammable gas that exists in atmospheric air at 0.5 ppm [30]. A hydrogen flame exhibits a faint bluish color that makes it difficult to detect even when burning. According to the Compressed Gas Association (CGA), hydrogen can burn in air at atmospheric temperature and pressure between 4 and 75 percent concentration with an auto ignition temperature of 566°C (1050°F). The minimum ignition energy is 0.02 mJ which means that static electricity discharge and stray sparks will be safety

considerations to the electrical system design. Other characteristics of hydrogen gas include its small molecular size which cause a high diffusivity in porous materials [30]. This means that hydrogen may leak out of a system that may be completely sealed for gasses of larger molecular size at equivalent pressure.

For the purposes of this system's design, it cannot be assumed that only hydrogen is within the system when idle for long durations. A purging process of inert gas (i.e., nitrogen) is necessary to achieve high quality hydrogen within the storage tanks and to avoid flammability limits at atmospheric pressure. This will ensure that the concentration limit for hydrogen flammability is never achieved within the system.

Other considerations suggested by the CGA to structural safety include hydrogen embrittlement. This can occur in metals and alloys. The three common means of metal embrittlement include environment hydrogen embrittlement by contact with high pressure hydrogen, internal hydrogen embrittlement due to absorbed hydrogen, and hydrogen reaction embrittlement. For these cases, hydrogen embrittlement will result in a loss of ductility, increase in surface cracks, and lower fracture toughness. For this reason, material selection is another important step for this system [30]. According to ASME B31.12, austenitic steels are strongly recommended as the most resilient type of stainless steel for avoiding hydrogen embrittlement in hydrogen gas piping and pressure vessels [33].

Hydrogen is primarily a flammability hazard. The flammability limit concentration is much lower than a hazardous asphyxiator concentration. A purge process will be completed every time the compressor is operated to further minimize the flammability limit of hydrogen gas for this system. The doors to the facilities will be open to atmosphere during any operation to allow ventilation as an added precaution.

B. APPLICABLE CODES AND SAFETY PROCEDURE

Because of the temporary nature of the system, many codes do not directly apply, but were taken into account in the design phase for the purpose of future scaling and added safety precaution. Title 29 of the U.S. Code of Federal Regulations (CFR) does not apply since station design was below of 11.3 m^3 (400 cubic feet) and 4536 kg (10,000 lbs.), but safety recommendations are followed for design purposes as per CFR 1910.103 for hydrogen storage

facilities. The Navy has its own standards that include Navy Occupational Safety and Health Program and Operational Risk Management. The design strategy followed Process Risk Management which incorporated removal of hazardous conditions, passive risk mitigation (not requiring operator action), continuously operated alarms and safety devices, and lastly, the use of standard operating procedures, inspections, and training to mitigate risk [13] [34]. Appropriate personnel must conduct these inspections to make the system permanent.

A purge process is used to expel contaminants from the lines to be within at least 99 percent hydrogen. This is well under the flammability limit which is four percent oxygen at atmospheric pressure. At atmospheric conditions, air consists mainly of oxygen and nitrogen at 21 and 78 percent respectively with traces of other gases amounting to the remaining percentage. The combustible region as shown in Figure 4 as the shaded region is defined by Crowl in *Understanding Explosions* as conditions that will support combustion [35]. The three sides of the triangle represent the main constituents of gasses as the residual gasses are assumed to be negligible. At any time within the triangle, the sum of the gasses will be at 100 percent within the triangle. There are a few options for the purge sequence to get from point F to point A described. The initial starting point of air is at point F with the goal of getting close to point A, pure hydrogen. CGA standards specifies that residual oxygen levels should be below 1 percent [32].

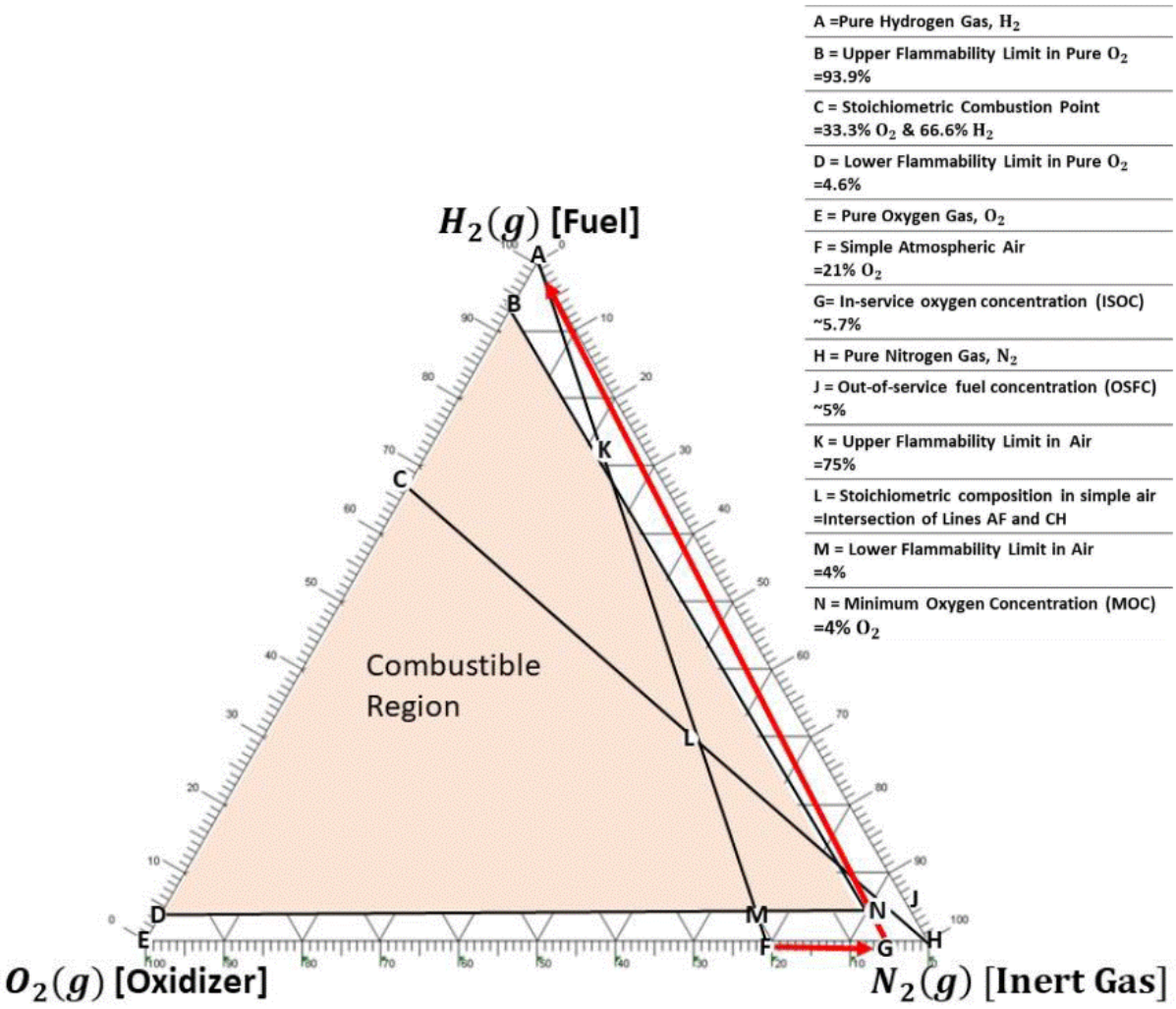

Figure 4. Composition Triangle Showing Purge Process for Oxygen, Nitrogen, and Hydrogen. Source: [13].

From the CGA, there are three purging methods that include sweeping of purge gas using inert gas, vacuum purging, or pressure purging with inert gas. A sweeping method was not used because there are portions of the facility, namely the containers that only have one inlet. Thus trapped contaminants will likely remain within the system. A combination of evacuation and pressure purging is equipped on the system to lessen the amount of purge gas required. Additionally, the EHC manufacturing company, Xergy, recommends this combination of purges to avoid degradation of the EHC cell membranes due to contaminants within the EHC operating manual. Crowl developed a formula in Equation 1 for the number of purge cycles required, *N*, which is related to the natural log of the ratio of concentrations

of oxygen, C_{safe} and C_{air}, divided by the natural log of the ratio of pressures within the system, P_{low} and P_{high}. C_{safe} was defined previously by the CGA as one percent and C_{air} is 21 percent for standard atmospheric conditions. P_{low} is the pressure achieved by vacuuming the system, and P_{high} is the pressure of the nitrogen purge gas. The purge procedure is discussed later in this chapter.

$$N \geq \frac{ln\left(\frac{C_{safe}}{C_{air}}\right)}{ln\left(\frac{P_{low}}{P_{high}}\right)} = \frac{ln\left(\frac{0.01}{0.21}\right)}{ln\left(\frac{P_{low}}{P_{high}}\right)}, N = 1,2,3, \ldots, \quad (1)$$

The design strategy addresses multiple features that reduce the flammability risk of the system. There are several continuously active measures including a low pressure relief valve, high pressure relief valve, and rupture disk for overpressure conditions. Additionally, all pressure releases that vent gas under normal operation will do so outside of the facility to reduce the chances of a combustible mixture. For automation and safety, a programmable logic controller is used to manage the facility. The programmed logic has an automatic shutdown procedure in the event of smoke detection or maximum pressure that is measured by sensors connected to the PLC. Lastly, there is manual control for shutdown of the compressor in both facilities.

Other practices of safety include proper grounding of the system to ensure no static charge builds on the piping system. Wiring is bonded and covered with electrical tape and heat shrink wrap or covered to prevent exposed contact with operator or piping system. The NFPA 2 is the applicable guidelines to wiring hydrogen systems. The current system abides by electrical area classifications for Class I Division 1, which states that electrical components should be beyond 1 m (3 ft.) of any vent outlet that is operated under normal conditions. However, due to the data collection and power leads to the compressor being exposed by design, a Class I Division 2 deficiency still exists as the vent outlet is within 4.6 m (15 ft.) of a hydrogen outlet. Because it is a Division 2 deficiency, the system must abide by NFPA 70 Article 501 which has additional rules that there should be “no uninsulated exposed parts operating over 30 V” that are exposed to hydrogen under normal operations [31] [36]. This system does not expose gas to the wiring under any normal operations, and there are no uninsulated parts operating over 30 V DC.

C. COMPONENT SELECTION AND IMPLEMENTATION

The following chapter will detail the systems used for the hydrogen production and storage facilities. The system is located at the NPS at the Turbopropulsion Laboratory. Solar panels were installed on the roof to maximize exposure to the sun in Monterey, CA. Outdoor sheds were chosen to house the components to maximize safety over an indoor installation. In the future, these sheds can be consolidated to a single Conex type shipping container that would possess the full operation and be easily transportable wherever energy generation and storage is necessary. The existing system is located at the outside building 216 as shown in Figure 5. Appendix A, B, C, and D respectively show the mechanical and electrical diagrams for the PV array, production shed, compression and storage shed, and control wire diagram.

Figure 5. NPS Hydrogen Compression and Storage Shed (left), Production and Control Shed (middle), and Capstone C30 Microturbine Shed (right)

1. Photovoltaic Array

The photo voltaic (PV) array is the power source of the entire operation. Previous work by Aviles [10] began this research effort by installation of solar panels and was furthered by Yu [11] with installation of panels on the roof of building 216 as shown in Figure 6. This was done to maximize solar energy production for the greatest amount of time to be exposed to the sun. A total of nine panels, as shown in Figure 6, were installed at this location. The total power output achieved was 2430 W at peak performance with three parallel strings of three solar panels in series as shown in Appendix A [11]. This power output is more than adequate at peak daylight times for all components presently to be integrated onto PV supplied power [11].

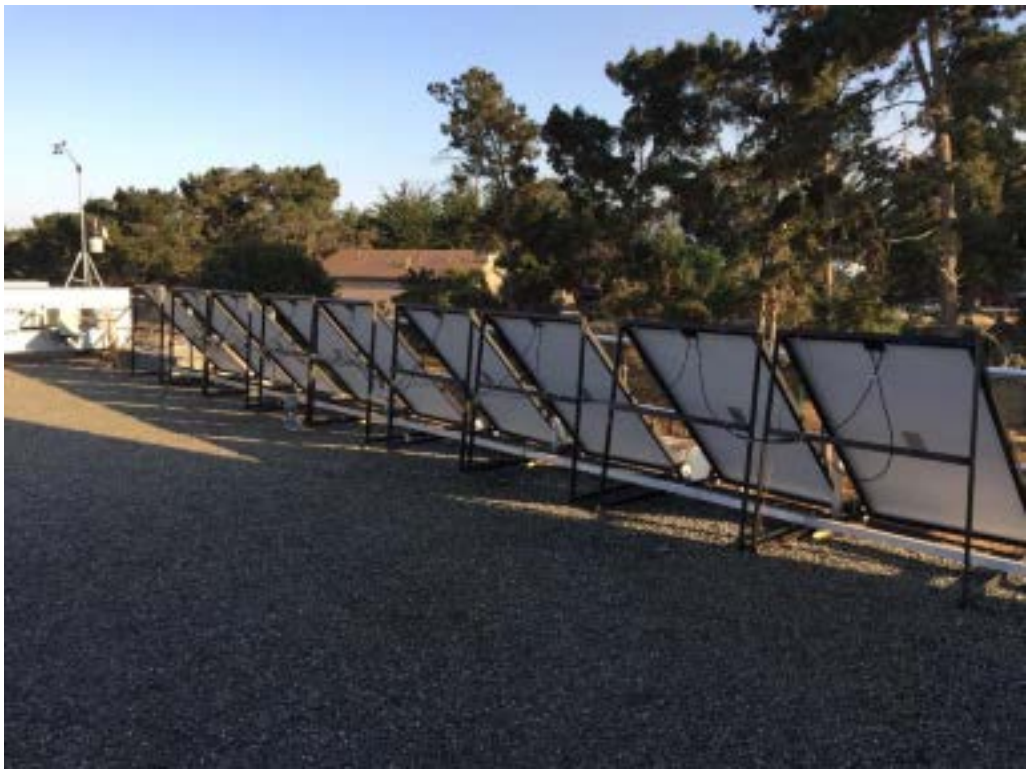

Figure 6. Solar Panel Array at NPS Turbopropulsion Lab, Building 216. Source: [11].

A Magnum PT100 charge controller, shown in Figure 7, is rated at 6600 W (well above maximum power output of solar panels) and has a maximum voltage of 187 VDC. The

magnum charge controller provides 12–13.6 VDC to the production system comprising of an electrolyzer and four dehumidifiers. A current transducer was added to the charge controller to track the power demand of the production shed at the charge controller input.

Figure 7. Magnum PT100 Charge Controller

2. Production System

The groundwork for the production system was completed by Aviles and Yu [10] [11]. There are four Ivation Peltier dehumidifiers that are used to collect moisture from the ambient air and drained into two storage tanks beneath them. The production rate was between 3 and 9 g/hr for each humidifier, and they consume about 77 W each [10]. Below the storage tanks are the process tanks containing a solution consisting of 15% potassium hydroxide (KOH) as the electrolyte. The process tanks are connected to the electrolyzer with two inlets and two outlets for both process tanks (Appendix B). The electrolyzer has an input for the KOH solution and separate outlets for hydrogen and oxygen. Hydrogen is pumped to the left side tank and oxygen is pumped to the right as shown in Figure 8. Its efficiency ranged

between 50 and 63 percent from Yu [11]. The system is gravity fed and the process tanks have exhaust hoses that will be led to the compressor for hydrogen and to atmosphere outside of the shed for oxygen. Work by Birkemeier has allowed for the initial production systems automation, but not integration with the compression and storage shed [12]. Piping has been installed to feed hydrogen to the compression and storage shed. Based on recommendations from Birkemeier, the original tank level indicators have been switched with a float type sensor that is integrated into the systems automation. Concurrent work is being done to replace the humidifiers with a 40 W units, but has not been tested for production rate at the time of this work's completion.

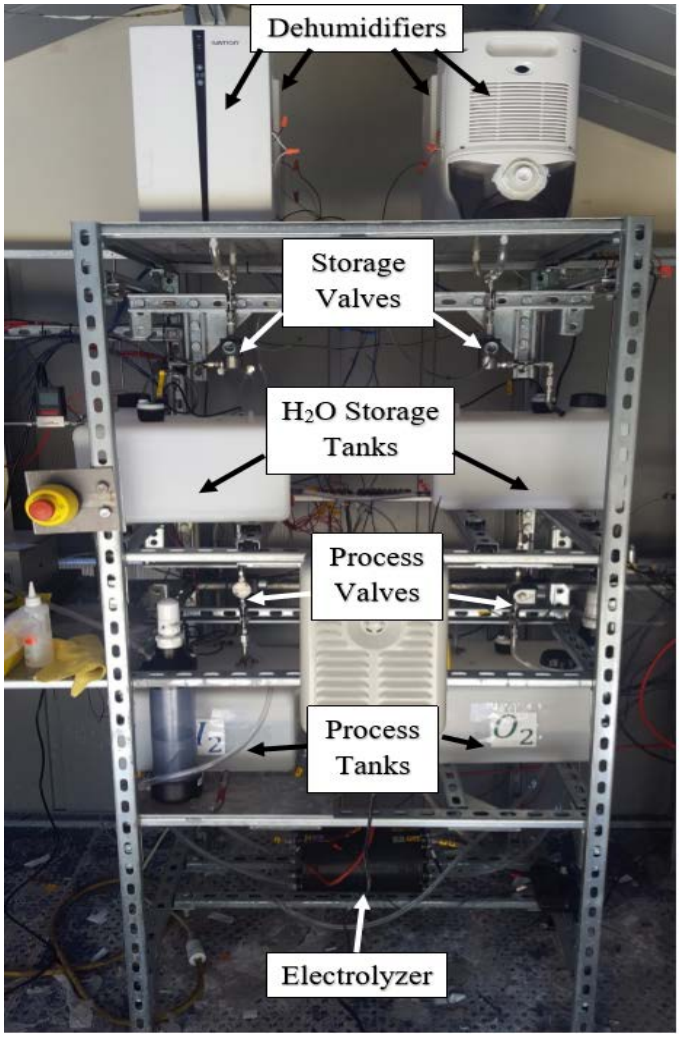

Figure 8. Production Plant. Source: [12].

3. Compressor, Piping, and Filters

Figure 9 shows the Xergy EHC devices that were tested in this work. The compressors have variable amounts of proton exchange membranes that correlate to increases in flow rate and required power. The first compressor has 16 cells and was rated to 10 bar by Xergy. The second compressor has 120 cells and was rated up to 34.5 bar. The last compressor had a single cell and was rated up to 103 bar. The devices have a circular cell pattern, and the voltage was monitored in testing to never exceed 500 mV per cell in the stack. The single cell compressor was recommended to run at 250 mV, per manufacturer's recommendations.

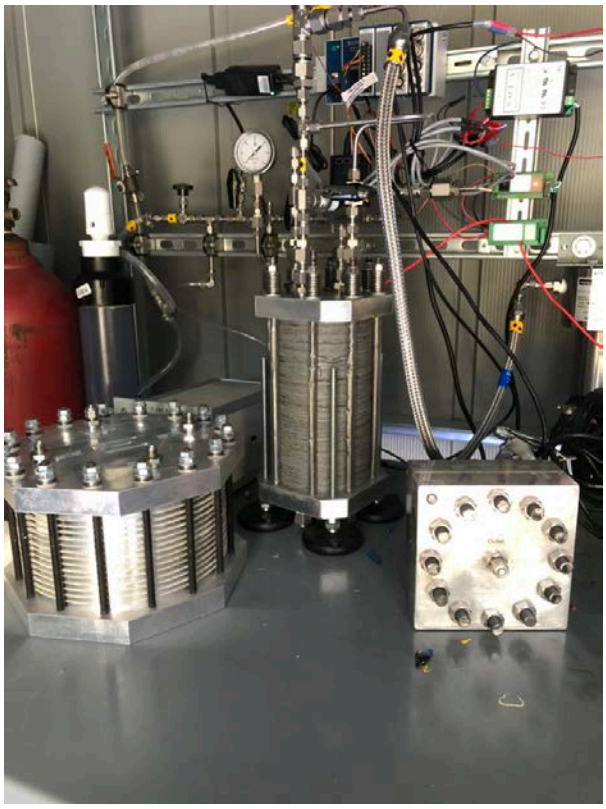

Figure 9. Xergy EHC 10 Bar Compressor (left), 34.5 Bar Compressor (middle), 103 Bar Compressor (right)

The EHC's performance can be evaluated by using the Nernst equation to determine the theoretical voltage across the cell that would give the output pressure based

on the input pressure. Using data collected for the cell temperature in Kelvin, *T*, and pressure ratio, p_2 and p_1, the theoretical voltage, and V_{theory} can be determined with the following constants in Equation 2: $\bar{R}$ as the universal gas constant (8.314 J/K.mol), *n* number reaction sites (two for diatomic hydrogen splitting), and *F* as the Faraday Constant (9649 C/mol). However, the cell temperature is approximated the average of the inlet and outlet gas since there is no internal thermocouple within it to measure the cell temperature.

$$V_{theory} = \frac{\bar{R} \cdot T}{n \cdot F} ln\left(\frac{p_2}{p_1}\right) \tag{2}$$

Nernst efficiency is calculated as this theoretical voltage multiplied by the number of cells, N_{cells}, in the stack and divided by the actual voltage measured becoming:

$$\eta_{Nernst} = \frac{V_{theory \cdot N_{cells}}}{w_{actual}}. \tag{3}$$

For comparison to Fosson's EHC models [13] and research done by Lipp, [18] calculations for the adiabatic and isothermal efficiency are included. EHC compressors follow an isothermal process, while mechanical compressors ideally track an adiabatic process. The next equation has the isothermal compression process efficiency. This is the ratio of ideal to actual specific work output, w_{ideal} over w_{actual}, which uses the temperature and pressure ratio as before with *R* as the hydrogen specific gas constant (4124.5 J/Kg-K) and γ as the hydrogen specific heat ratio (1.4065) [13]. The Also, included for the actual work is the compressor power,P_{total}, and the mass flow rate, $\dot{m}$ (kg/s) are also included for actual work in the next equation:

$$\eta_{adiabatic} = \frac{w_{ideal}}{w_{actual}} = \frac{\frac{\gamma}{\gamma-1} RT_1 [\left(\frac{p_2}{p_1}\right)^{\frac{\gamma}{\gamma-1}} - 1]}{P_{total}/\dot{m}}. \tag{4}$$

Next, the ideal isothermal efficiency can be calculated by using the hydrogen gas constant, inlet temperature, and pressure ratio again compared to the actual work as

$$\eta_{isothermal} = \frac{w_{ideal}}{w_{actual}} = \frac{RT_1 \, ln\left(\frac{p_2}{p_1}\right)}{P_{total}/\dot{m}}. \tag{5}$$

The electrochemical compressors require that the hydrogen fed by the production plant is humidified. This was accomplished by passing the hydrogen through a bubbler as

shown in Figure 10. This, which also prevents particle contaminants from seeping into the compressor. The bubbler has a spring actuated overpressure relief opening that will activate at approximately 2 bar (30 psi).

Figure 10. Bubbler for Humidification of the Hydrogen Working Fluid with a Low-Pressure Release Valve

The low pressure lines feature a plastic-clear line with a diameter of 9 mm (0.375 in.) and was sufficient for the production plant flow rate. This line runs from the production shed to the compression and storage shed. There are two external events that are manually operated to drain moisture from the line if necessary. When inactive for periods of more than a few hours, the lines should be purged with the hydrogen working fluid, or gaps will

inevitably allow hydrogen to escape and oxygen to enter. The distance between the sheds is not optimal in this regard. The current design would only allow for a sweep purge of hydrogen to purify the line. This requires a substantial amount of hydrogen to flow through the line to reduce the residual air to the desired concentration.

Swagelok parts were chosen for the supply of high pressure piping and valve equipment. They offer mechanical compression fittings that allow for the system to be modified and refit to accommodate changes in the design of the system. Swagelok parts conform to ASTM A213, which means that it meets the standardized processes for stainless steel pressure tubing. The equipment used in this project consists of needle valves, ball valves, fittings, joints, 6.35 and 12.7 mm (0.25 and 0.5 in.) piping with a system rated pressure of 207 bar (3000 psi). The check valve previously installed by Fosson was removed to allow for the purge cycle to effectively purge the entire system. A rupture disk, a passive pressure safety device, was previously installed to break at a pressure of 207 bar (3000 psi). A proportional relief valve (PRV) adds redundancy as another passive measure to prevent overpressure. It was modified by changing a setscrew to the desired pressure of 150 bar (2175 psi), which prevents overstressing any high-pressure components. The setscrews are interchangeable for further system refinements. These valves are shown in Figure 11. The pressure differential between the inlet and outlet of the compressor should not exceed the manufacturer's recommendation to avoid leaks forming within the cell of the membrane. Another precaution is that the compressor membrane will not be exposed to high pressure when the compressor is not running. This will require operator involvement to vent the high pressure lines until automatic control valves are implemented.

Figure 11. Rupture Disc (left) and Proportional Relief Valve (right) Overpressure Safety Systems

4. Storage Station

Once the hydrogen exits the EHC, it passes through a bulk fluid separator for the water particles (media type 100 W) to be separated from the high-pressure hydrogen gas. This must be periodically drained through the bottom, as the element eventually fills up. The device consists of metal retainer with a rolled mesh screen to separate the liquid all within the 414 bar (6000 psig) rated stainless steel housing. The second device is the Parker SJ-Series filter which is also rated up to 414 bar (6000 psi) with a 316 stainless steel construction. It has similar construction to the separator but has a fine filter for media grade A, which removes hydrocarbon vapors or other particles with a Micron rating of 3. These filters shown in series in Figure 12 may require ongoing maintenance over time to drain with an accessible port at the bottom of the housing [37].

Figure 12. Parker High Pressure Filters

From Fosson's work, six hydrogen (red) and four nitrogen tanks (black) were installed as shown in Figure 13. The maximum pressure to transport the cylinders is dictated by the Department of Transportation at 156.2 bar (2265 psi). The 32.2 L cylinders are placed in parallel service with a common manifold to enable simultaneous filling or discharge if desired [13]. Further additions for piping line to a turbine or fuel cell are available at either side of the tanks. The capacity of the hydrogen station is shown on Table 2 for single cylinder and six-cylinder use. The pressures compare to EHC values or the maximum DOT tank pressure. The nitrogen storage tanks supply the inert purge gas used to reduce the atmospheric oxygen concentration to below flammability limits. A pressure regulator is available to change the high pressure of the purge process according to the desired purge process from Equation 1.

Figure 13. High Pressure Hydrogen Storage Tanks (left) and Nitrogen Storage Tanks (right)

Table 2. Hydrogen Capacity at Various Pressures

Pressure, bar (psig)	H_2 single-cylinder, kg	H_2 six-cylinder, kg
4.62 (67)	0.015	0.092
10.3 (150)	0.034	0.207
34.5 (500)	0.115	0.690
103 (1500)	0.344	2.064
156.16 (2265)	0.520	3.123

A vacuum pump is attached to the high-pressure side as a part of the purge cycle. The vacuum is located after the water separator to prevent degradation of the pump due to moisture. A vacuum pump will save on purge gas by reducing the number of cycles required through the purge process especially when multiple cylinders are used. The sacrifice of power to drive the vacuum device will be dependent on the availability of purge gas. Utilization of both purge gas and vacuum pump or either of the two could be used to achieve the same result. Sensors and Data Collection

A summary of the sensors used is shown in Table 3. A combination of analog pressure transducers and pressure gauges are used in the compression shed. The production shed utilizes the Allen Bradley Micro 850 Programmable Logic Controller (PLC), as shown in Figure 14, and is programmed through Connected Components Workbench (CCW) software. Updates to the PLC can be accomplished on location using an Ethernet connection to a PC. The Micro 850 has a 24 point input output interface with lead options for additional modules. The PLC's code from CCW software is shown in Appendix D. This software is programmed directly to the controller using an Ethernet connection to a PC. Add-ons are available to the Micro 850 that allow for conversion of analog input ports within the PLC program. These modules include two 2080-IF4 modules (four analog input ports) and one 2080-OF2 (two variable analog voltage outputs). Other expansions include the OF4 and OB16 which have 4 analog outputs and 16 digital output ports, respectively. Any further automation beyond this thesis may require a separate controller or additional plug-in modules for the compression and storage shed.

Table 3. Summary of Sensors Used

Sensor	**Value(s) Measured (Range)**	**Output**
Alicat M-series Flow Meter	Flow rate (0.001- 1.600 slpm), Pressure (0-13.8 bar), Temperature (-20-70 °C)	USB serial
Honeywell MLH Series 500 psi Pressure Transducers	Pressure (0-34.37 bar)	0.5-4.5 V
Honeywell Pressure MLH Series 3000 psi Transducers	Pressure (0-206.84 bar)	0.5-4.5 V
HYME Hydrogen Gas Analyzer	Hydrogen Purity (80-99.99%)	4-20 mA
Current Transducers	DC Current (0-50 A)	0-10 V
Tank Level Sensors	Tank Level (0-4.5 in.)	0-5 V

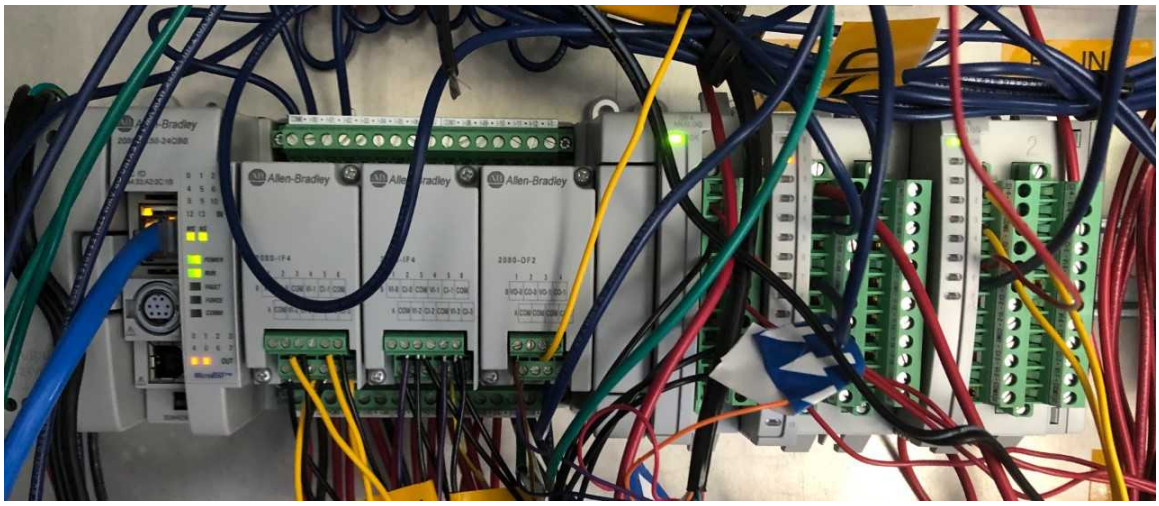

Figure 14. Allen Bradley 850 Microcontroller. Source: [12].

Solid State Relays (SSR) were used to control the power to essential functions of the system including the dehumidifiers, electrolyzer, and compressor. The complete electrical diagram from Birkemeier's work [12] on the system is shown in Appendix E. SSR's will not spark when activated and are very reliable with no moving parts. In this work, a DC SSR was integrated into the EHC as a shutoff from the production shed. This also prevents exposure to hydrogen in the event of a gas leak. Another DC SSR was used for the EHC.

Data acquisition (DAQ) for the storage facility was accomplished using the National Instruments Compact DAQ Model cDAQ-9184 with two analog voltage inputs for temperature, two analog voltage inputs for pressure, voltage sensor across compressor stack, a current transducer, and a voltage sensor scaled for PV power from the PLC. The Alicat M-Series mass flow meter for hydrogen recorded the flow rate. This was integrated with the DAQ through a universal serial bus (USB) serial connection to a PC running a MATLAB script that records both the DAQ and USB serial connection from the flowmeter. The data capture and subsequent data reduction are shown in Appendix F and H, respectively.

5. Controllable Valves

Controllable valves are implemented in this research for the operation of the hydrogen production unit. These have normally closed logic and are electrically operated with the PLC microcontroller. A proportional integral derivative (PID) controlled valve was also programmed to open and close the oxygen exhaust valve to keep the process tank liquid levels approximately even. An additional controllable valve was added to vent excess hydrogen on the production side to prevent over pressurization of the tank since EHC compressors can have a significantly low flow rates compared to the minimum electrolyzer output.

D. SYSTEM OPERATION

1. Start-up

A procedure was developed to ensure the high quality hydrogen is stored while maximizing the lifespan of the EHC. The standard operating procedure given by Xergy was modified for the NPS system to follow the calculated purge cycle. The controller uses logical statements (Appendix E) based on available PV voltage to control how many humidifiers are operating and is programmed to maintain level tanks through opening valves. The electrolyzer current can be set to match the expected flow rate of the compressor. When there is sufficient solar power to start the electrolyzer, the hydrogen will flush the low-pressure hydrogen line. This takes approximately 45 minutes for the electrolyzer to flush the low-pressure line and attain hydrogen purity above 94–96 percent according to the gas analyzer. Since the gas is humidified by passing through water, the remaining percentage is due to the concentration of water vapor that is a function of the temperature.

Once the production system is purging the line, the high-pressure lines must be purged in accordance with the CGA guidelines to avoid the flammable region. The chosen method for purging is a combination of pressure and vacuum purging from Equation 1 where the high pressure is given as 2.06 bar (30 psig) supplied nitrogen. To minimize the cycles to one, a vacuum is chosen to lower the absolute pressure to 0.04 bar (or measured relative pressure of 28.5 inHg). The primary method of reducing the oxygen concentration

required the following steps: vacuuming the entire compression station, opening nitrogen regulator valve to 2.06 bar (30 psig), vacuuming again to 0.04 bar (28.5 in Hg), and filling with hydrogen to at least atmospheric pressure. Other practical combinations with and without the vacuum pump and purge gas are shown in Table 4. These three options are optimized to reduce the number of cycles and amount of purge gas. Once the system is purged and the gas analyzer shows that 94 percent pure hydrogen is at the inlet to the system, hydrogen fills the system to atmospheric conditions of at least 1.01 bar (0 psig). The bypass of the compressor must be shut off, and the EHC button safety switch pressed to change the relay for the compressor, which is set for constant voltage mode, not exceeding the maximum stack voltage as dictated by the operating manual. At this point, data collection was started manually for a designated time as shown within the MATLAB Code from Appendix F. A simplified version of the compression system from Appendix C is shown in Figure 15 with gas analyzer, flowmeter, relay, filter, separator, and vacuum pump.

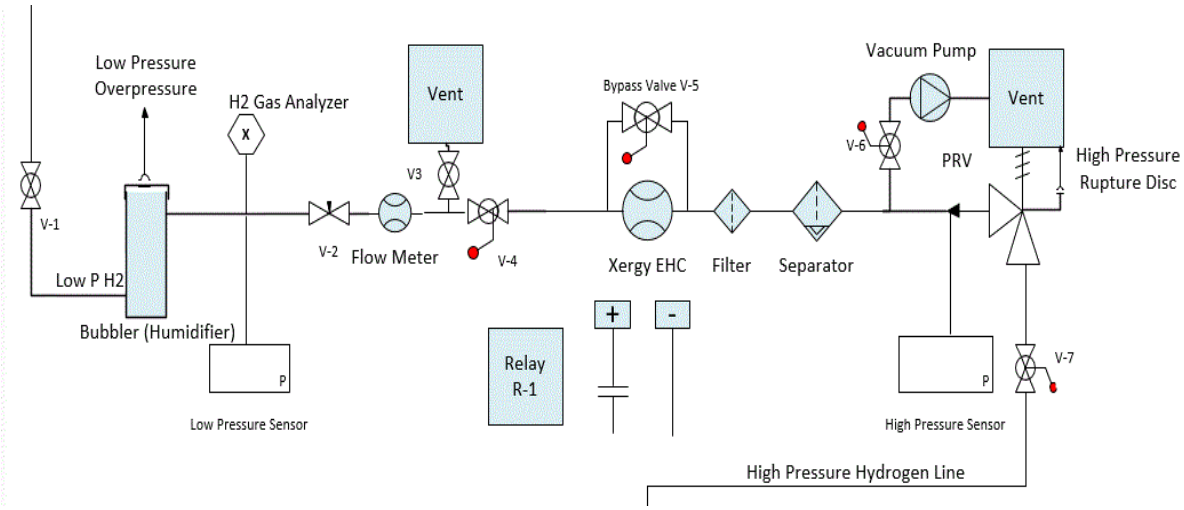

Figure 15. Compression System Diagram

Table 4. Purge Pressure Combinations

Method	P_{low}, bar (inHg relative)	P_{high}, bar (psig)	Cycles, N	N_2 Purge Gas, kg
Purge Gas and Vacuum	0.04 (28.5)	2.06 (30)	1	0.6
Purge Gas Only	1.01 (0.00)	3.03 (44)*	3	1.8
Vacuum Only	0.04 (28.5)	1.03 (14.7)**	2	0

*~99% Nitrogen at system start (lower hydrogen quality)

**Must be hydrogen supplied for the high pressure

2. Steady-State Operation

At steady state conditions, the only necessary modifications to be made to the compressor voltage will be if the compressor inlet vacuum pressure is too high on the process hydrogen tank by raising the fluid level to exceed the tank limits. This will need to be addressed by the design of the buck converter for integrating the compressor under the PV array power. The tank levels are regulated by PID valve on the oxygen side and a blow off valve on the hydrogen side if excess hydrogen is being produced. An alternative design would be to stop and restart the electrolyzer or compressor, but the effects on hydrogen purity should be evaluated before changing the code.

3. Shut-down

An operator is not required to shut-down when there is insufficient solar power for the electrolyzer. As an added precaution for EHC durability, the tanks were manually closed and the high-pressure lines were vented to outside air before the EHC power was shut off. This was done to prevent leaks from forming within the membrane when there was no power supplied. There are several automatic shutoffs contained within the PLC operation. If the pressure on the system reaches the set pressure as measured by the transducers, the relay for the compressor will be shut-off. Once below the threshold of power available to the electrolyzer, the relay will be shut-off. The manual switch for the compressor may also be depressed to disengage the relay. In addition to these, the PRV valve and the rupture disk also

provide mechanical redundancy to release the pressure if it goes beyond their respective thresholds.

THIS PAGE INTENTIONALLY LEFT BLANK

III. TESTING AND ANALYSIS

A. PRODUCTION TESTING AND DISCUSSION

Tests were conducted to analyze the performance of the production facility. The first test was to characterize the flow rate of the electrolyzer by varying the current. The electrolyzer must produce hydrogen at a higher rate than the compressor to avoid a vacuum within the system. This may allow contaminants from the air to enter the low pressure line and cause the process tanks to be uneven. Since the electorlyzer's installation, there is a performance drop of about 0.1 slpm across the power band compared to Yu after two years of operation [11]. The relationship between the production flow rate in slpm and power in watts is shown in Figure 16. Measurements were taken using the display screens of the charge controller and electrolyzer current with verification using a voltmeter. The maximum pressure of the process tanks was measured to be approximately 1.2 bar before leaks would form in the seals.

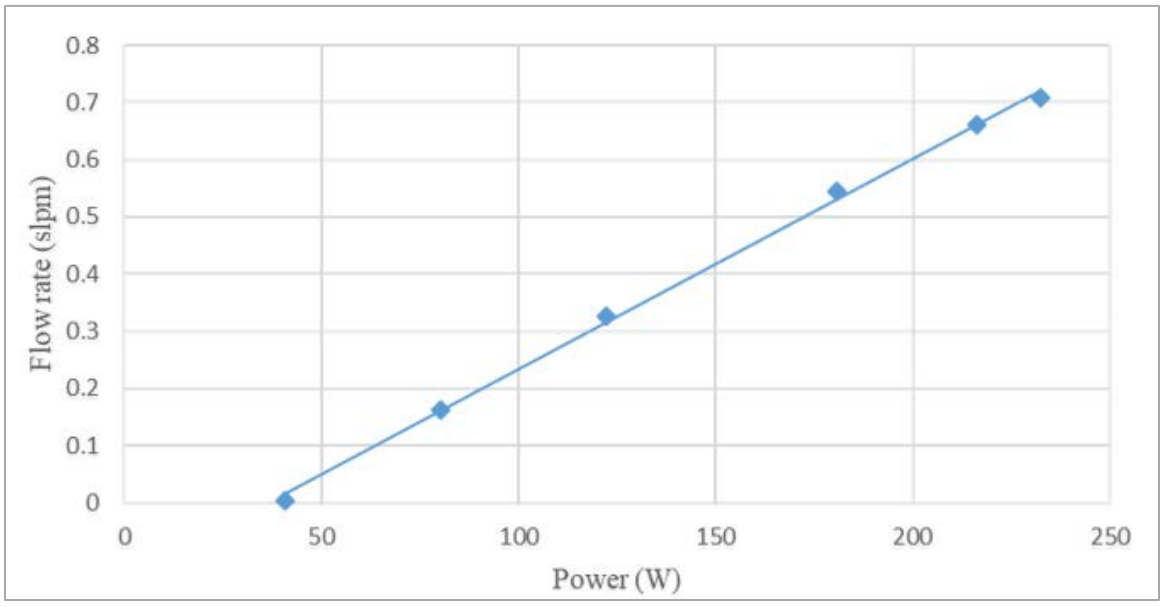

Figure 16. Electrolyzer Power vs. Flow Rate

The next test completed was a power consumption analysis of the humidifiers, which make up the other elements that consume power in the system. They consume about 77 W each, but a replacement upgrade will be 40 W dehumidifiers that have higher projected water output. Small openings near the top of the shed may also increase the effectiveness of the humidifiers to maintain the ambient relative humidity within the shed. From Yu's testing, the average production rate was 5.6 grams per hour [11].

PV max power performance without the compressor was already completed by Yu [11]. With limited PV power there are occasional sudden drops in power recorded by the PLC that may cause the system to malfunction if the system is fully isolated from the grid. A characteristic PV power drop that could lead could lead to loss of control in the system is shown in Figure 17 when PV power drops significantly over a 12 second window.

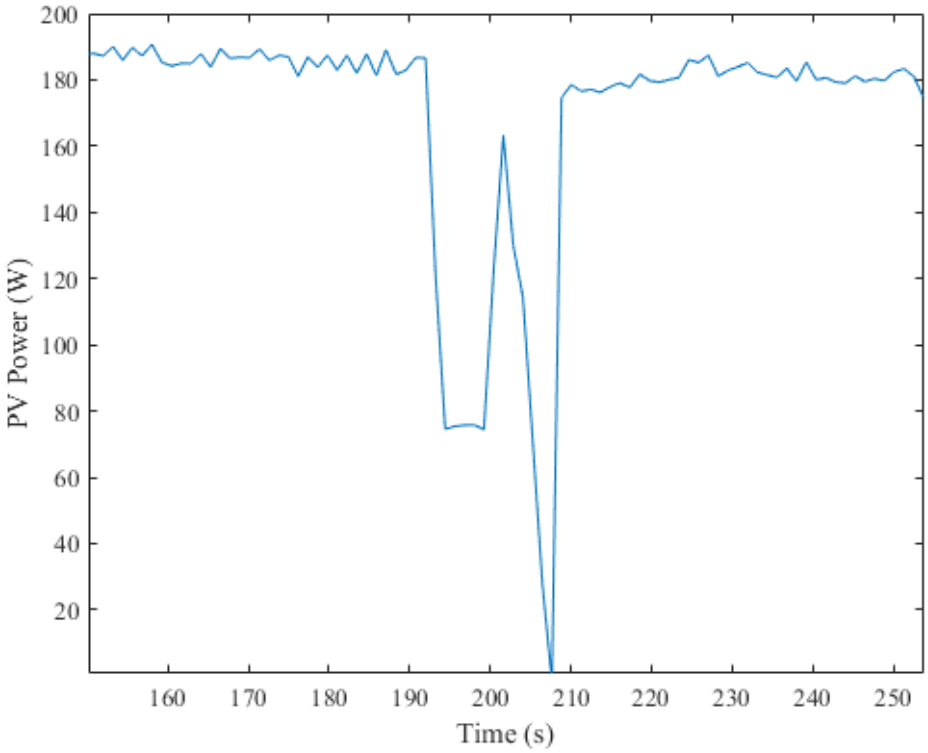

Figure 17. PV Power vs. Time of Run

B. COMPRESSOR TESTING AND ANALYSIS

In previous work by Fosson [13], two EHC compressors manufactured by Xergy were tested. This included a small 15 cell compressor consuming 5–15 Watts and a 4.0 slpm, 120 cell compressor which had a higher power rating. During initial testing, the 0.4 slpm compressor achieved pressures as high as 34 bar (500 psi) in testing before a catastrophic failure due to an internal leak. The 120 cell compressor also failed during its initial testing around 4.5-5 bar. Though both devices failed, the relatively low power consumption and projected pressure ratings made them viable for further testing with this work. The reason for failure may have been caused by a design flaw or a faulty procedure that allows the membrane to be exposed to high pressure when no power is supplied. For this research, three compressors were tested shown in Figure 9 from the previous chapter. The first compressor was also a 16 cell compressor rated up to 10.3 bar. This compressor failed on its initial testing phase before data could be collected. It was over-pressurized causing a massive internal leak within the system similar to previous failures. The second compressor tested was the rebuilt 120 cell compressor from Fosson's work and achieved a maximum pressure of 5.17 bar (75 psi) consistently with an average power consumption of 31.7 W. However, this compressor only achieved a fraction of the original rated pressure, which is between 21–34 bar (300-500 psi). The last compressor tested had a single cell and average power consumption of 1.38 W. This EHC was only tested up to 34.5 bar, but is expected to deliver a 103 bar (1500 psi) at a very low flow of 0.01 slpm according to Xergy.

1. 120 Cell, 21–34 Bar Rated Compressor Testing

The use of EHCs will generally not accomplish a steady state pressure, but will continue to rise until the membrane ruptures or the current drops to zero. The first test on the rebuilt 4.0 SLPM compressor was to find the flow rate at specified constant voltage points as shown in Figure 18. Matching the flow rate of the production shed is critical to ensure no hydrogen is exhausted unnecessarily during operation. This will inevitably occur if production exceeds the compressor's flow rate. The compressor was tested using constant voltage mode in contrast to Fosson's research [13] that used constant current.

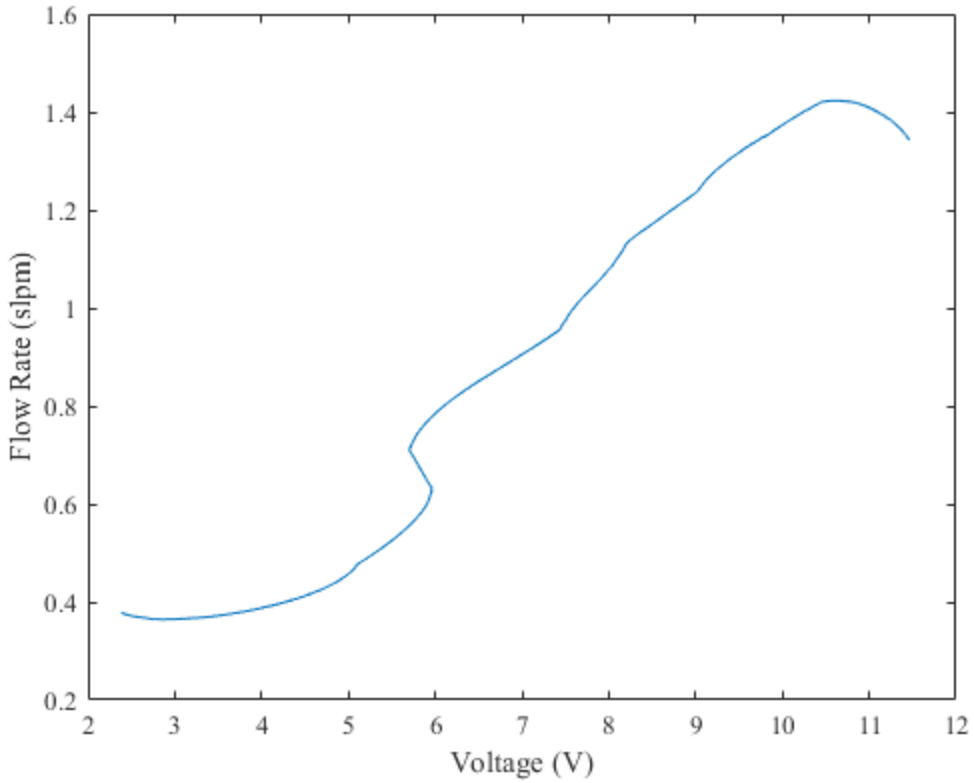

Figure 18. Flow Rate vs. Compressor Voltage

The next tests were steady state tests to verify the behavior of the compressor over time as pressure builds within the storage system. A single 0.15L pressure tank was used for this test. A characteristic plot in Figure 19 shows how the pressure and flow rate behave as they reach steady state. The data was smoothed using the Savitzky-Golay filter with a frame length of 100 data points in the MATLAB post-processing script (Appendix G). The outlet pressure starts to asymptote at its maximum pressure of about 5.5 bar, and the flow rate drops as fewer protons pass through the exchange membrane. The compressor, since it was rebuilt, does not come close to its rated pressure which was originally 21–34 bar (300-500 psi). However, it has a much higher flow rate than the 103 bar compressor, which may make it more desirable to incorporate with other compressors to maintain the highest possible flow rate for the pressure in the tank.

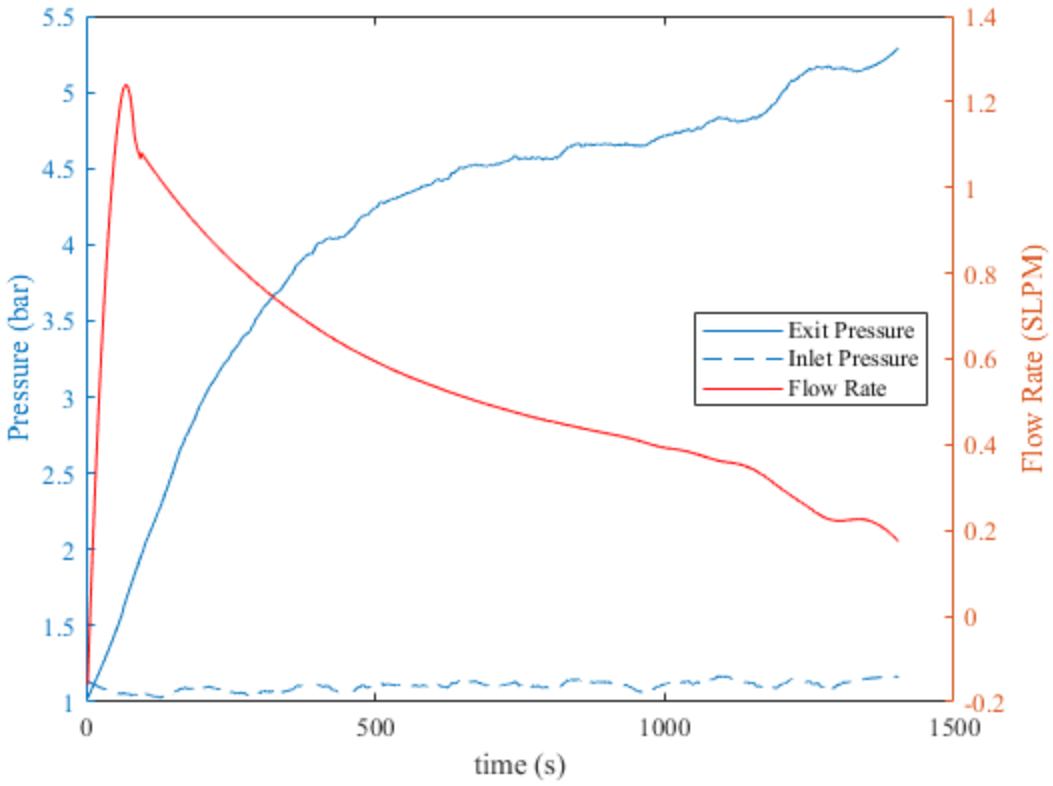

Figure 19. Pressure and Flow rate vs. Time

From equations 3, 4, and 5, the efficiency of the compressor was tested showing peak performance for the isentropic process and adiabatic process at 3.75 bar in Figure 20. The isothermal and adiabatic efficiency at this pressure are 13.4 and 16.1 percent, respectively. The Nernst Efficiency asymptotes as the pressure ratio stabilizes. Since there were 120 membranes, only a fraction of these cells had a significant voltage potential (>100 mV) when individual cells were sampled with a voltmeter probe. Therefore, 50 cells are used to calculate Nernst efficiency. This behavior is typical of most EHCs in that the individual cells have more potential across them towards the negative lead to the power supply.

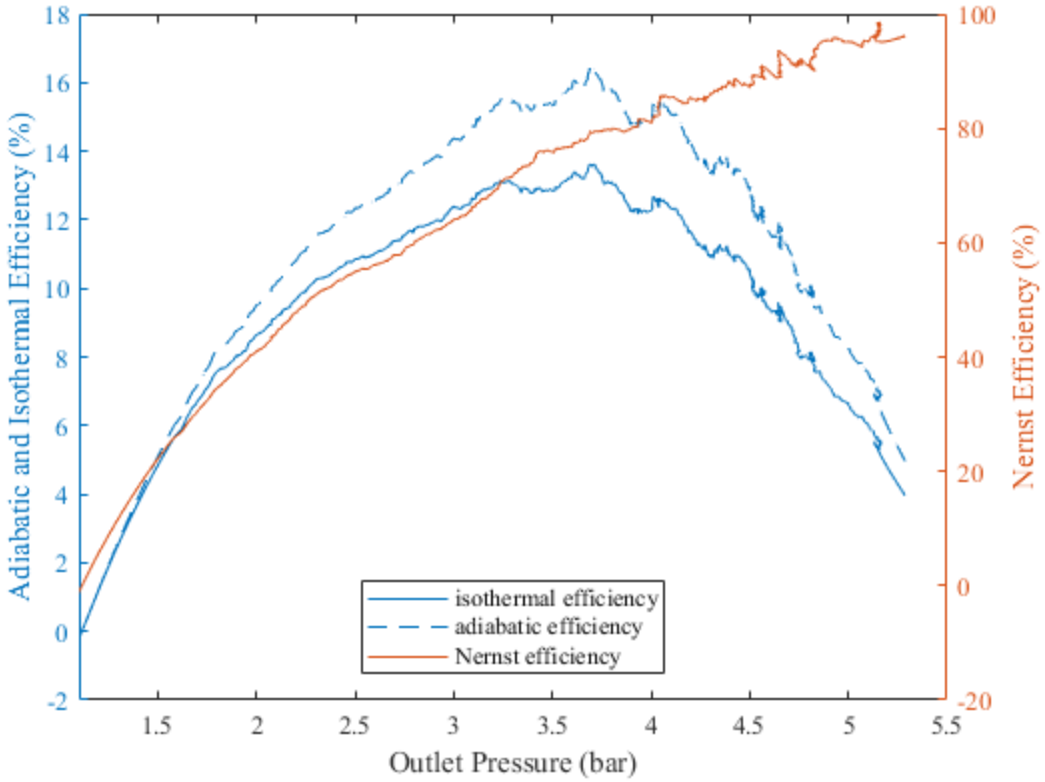

Figure 20. Efficiency vs. Outlet Pressure

2. 1 Cell, 103 Bar Rated Compressor Testing

The 103 bar compressor operates at an extremely low flow rate, current, and voltage. Reading data at this level was especially noisy as it was almost out of range for many of the sensors installed. As was the case with the 34.5 rated compressor, the start-up voltage has a characteristic flow rate. Even with a data smoothing function, there are still uncharacteristic drops recorded in the flow rate as shown in Figure 21. The flow meter is located 0.1 meters upstream of the inlet and is operating near the minimum limit for flow rate measurements. The maximum suggested voltage of 250 mV was used for this single cell compressor for further steady state testing.

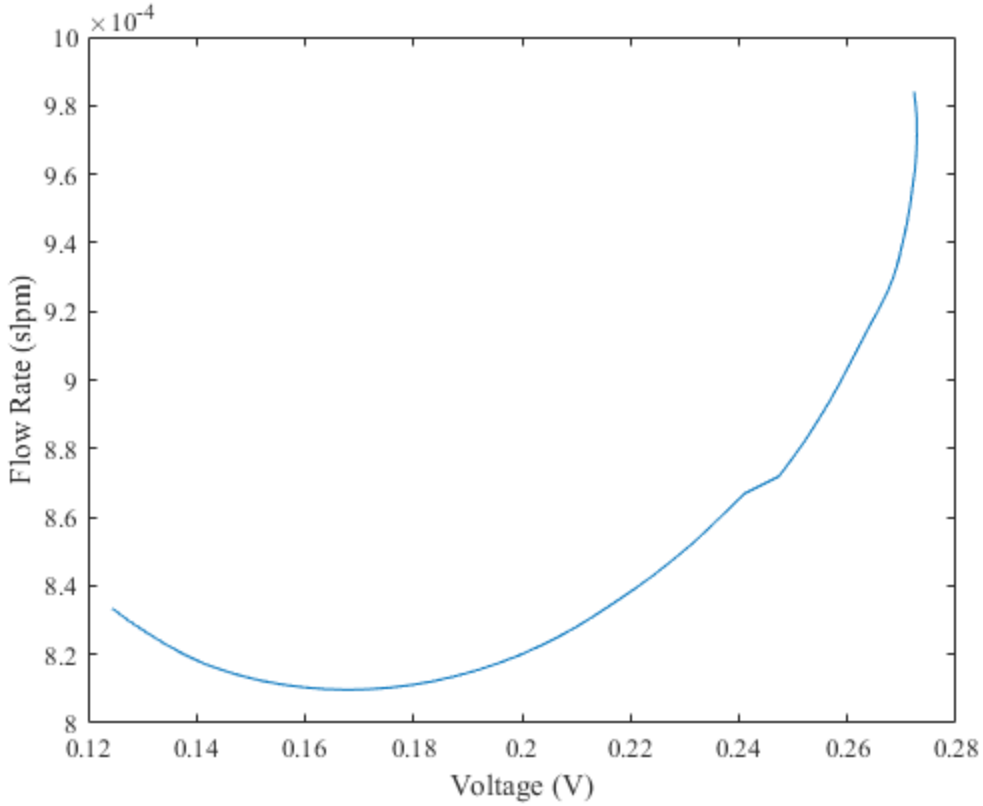

Figure 21. Flow Rate vs. Compressor Voltage

The next tests were steady state tests to see the behavior of the compressor over time as pressure builds within the storage system. Since the flow rate was very low, only a small pressure vessel was used (approximately 0.01 L). A characteristic plot in Figure 22 shows just a small window into the compressor's capability. The average flow rate at this operational pressure is approximately 0.004 slpm which is more than two orders of magnitude lower than the minimum production rate. Since the inlet process tank is only rated to 1.2 bar, the electrolyzer must shut-off in order to maintain constant process tank levels. The steady linear increase in pressure predicts a much higher capability for further tests. To put this into perspective, it would take about 7100 hours of operation to fill the 32.2 L storage facility to 34.5 bar, storing only 0.69 kg of hydrogen.

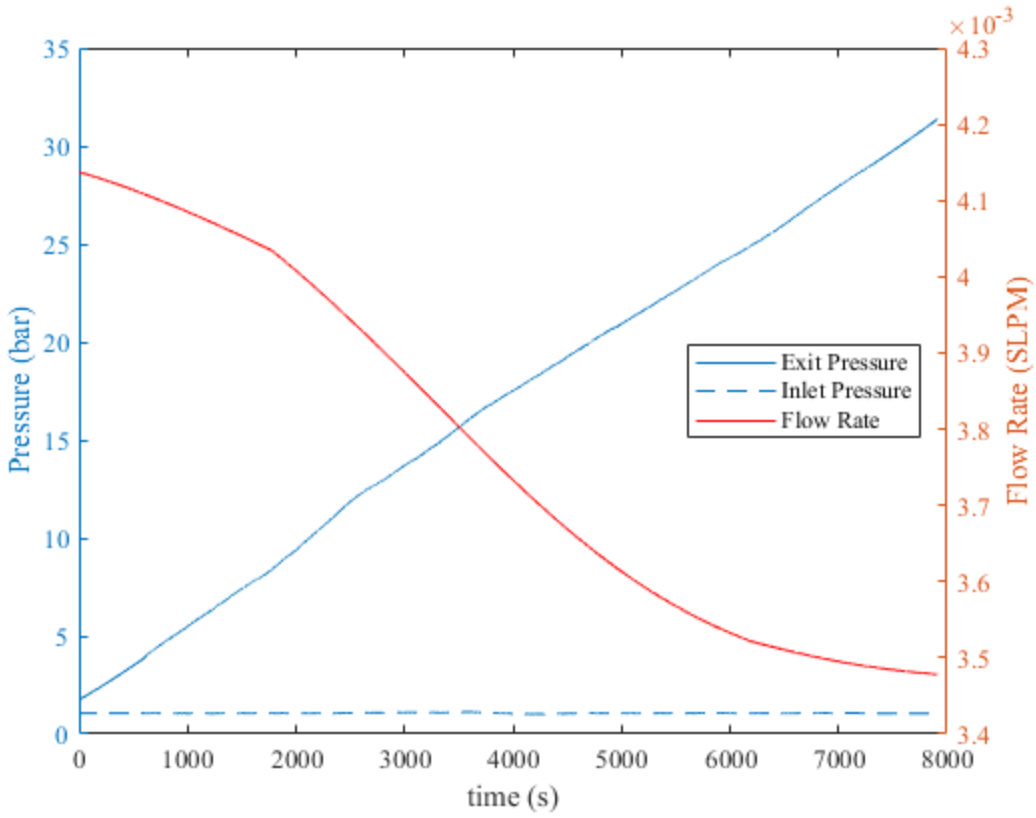

Figure 22. Pressure and Flow Rate vs. Time

Lastly, the adiabatic, isothermal, and Nernst efficiencies were evaluated. Similarly to Fosson [13], the adiabatic and isothermal efficiencies are extremely small. The maximum efficiency was not captured over this pressure range and will require further testing at higher pressures. Since all the efficiencies are functions of the pressure ratio, they are likely to continue to rise until the mass flow rate drops as the EHC reaches its maximum achievable pressure. The maximum pressure for the hydrogen storage tanks at 156.2 bar (2265 psi) is achievable if the EHCs are installed sequentially as long as the inlet and outlet differential is only 103 bar (1500 psi). The trade-off between high pressures and high flow rates is a major hurdle of the EHC design for a production and storage station. For storing the maximum amount of hydrogen in the least amount of time, it would be desirable to be able to switch between compressors that have different operating regimes. For example, the 120 cell EHC could operate until its maximum pressure is reached. Then a single cell could be powered to further increase the pressure but at a lower rate. Depending on the

demand frequency for the compressed hydrogen, pressurizing the storage system to its limit may not be necessary. However, the station should maximize the production rate by increasing the flow rate at each stage being careful not to exceed the electrolyzer output.

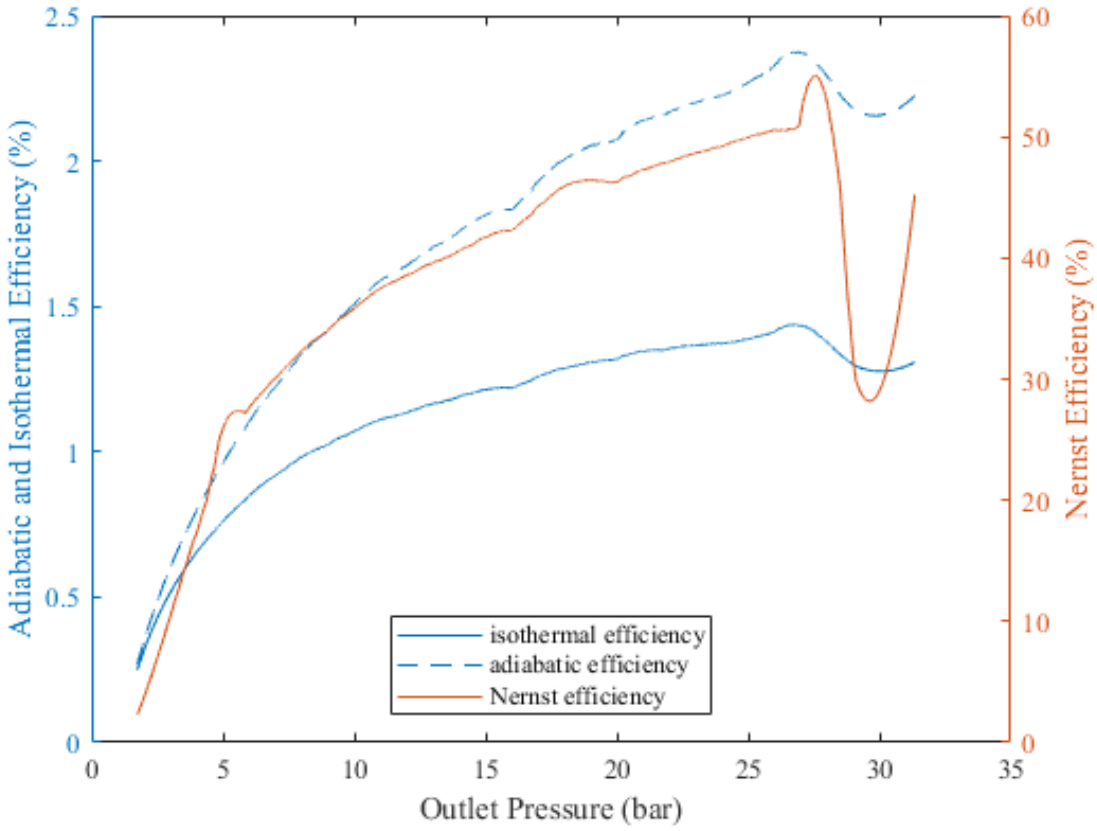

Figure 23. Efficiency vs. Outlet Pressure

THIS PAGE INTENTIONALLY LEFT BLANK

IV. CONCLUSION

A. SYSTEM PERFORMANCE

The system in place produces renewably sourced hydrogen and is capable of storing the hydrogen in tanks for future use in a fuel cell or a gas turbine. The purge process is effective in ensuring proper safety within the facility. Many safety measures, both passive and active, are set in place for system operation without operator involvement. The compressors remain the most significant challenge to the system's overall performance. With another step in automation, the process can effectively run autonomously making the low flow rates of EHC compressors an ideal choice for this system. Since the EHCs are the limiting step in the design loop, the system will improve significantly as the technology matures and evolves.

Many improvements to the production facility are necessary to accommodate the compressor, which include more robust control logic for improved performance, updated tank level, improved dehumidifiers, high pressure filters, and purge processes. The system can operate autonomously once started and even stop itself if necessary using the PLC.

The implications of this research will benefit shore installations that already have renewably sourced energy. At peak production times, instead of shutting down the renewable source, a system such as this could be powered up for future use as a primary source or even emergency power if there is a grid failure. The other potential benefactor will be DoD operations utilizing hydrogen fuel cell drones. With a forward deployed production facility in the size of a shipping container, UAV or UUV drones can have minimal logistical support once the system is in place and have extensive range once in theater.

B. RECOMMENDATIONS FOR FUTURE WORK

Based on the results of this work, there are a few steps necessary to improve and automate the entire renewable energy storage operation. It is recommended that another compressor of moderate flow rate of about 0.4 to 1.4 slpm and 34.5 bar pressure rating be added to the existing compressors. This configuration will optimize the production rate and

maximum pressure so that the inherent trade-off of flow rate and pressure rating has less of an effect in total hydrogen production.

In the future it will be necessary to add high pressure actuated valves to automate the purging process, close the tanks, open/close the bypass valve, and exhaust residual gas in lines. Pneumatic-electric valves will require additional compressed gas to operate the valve and are not the primary choice for future design. Fully-electronically operated valves may require relays depending on the power consumption. The power requirement must be low so as to not exceed the maximum power of the controller, and these valves only require power when switching. In order to maintain a system rating at 206 bar (3000 psi), these valves tend to have high costs at this pressure. A suggestion for the minimum amount of controllable is shown in the mechanical diagram of Appendix C. With a second controller, the two PLC microcontrollers can act independently or together. If they were to act independently, the compressor and storage shed PLC would use a hydrogen purity sensor requirement as the conditional to start the operation. A satisfied pressure condition or minimum PV power will initialize the shut-down procedure.

Data acquisition can also be replaced with the microcontrollers using the program, ControlLogix instead of the current DAQ that requires manual startup. By configuring the Micro 850 with additional modules, the current DAQ measurements can be read the analog voltage inputs. EHC data collection currently uses building power as its supply. Additionally, the compressor must use the power supplied by the PV array to accomplish the goal of self-sufficiency. The PV array has the capability to achieve the EHC power requirement, but it will require additional work to step down the voltage from the PV array voltage to the EHC desired voltage and controllers.

To prolong operation and maintain a back-up supply of power for shut-down, a battery or capacitor could be used to capture excess PV power. This would prolong the production time at the end of a day and steady the system when heavy cloud cover can significantly reduce available power. The back-up supply will ensure that the system can safely shut down by closing the storage tanks and venting the lines using controllable valves for EHC shut-down.

Small holes in the production shed may improve dehumidifier performance as the relative humidity will remain constant through mixing with outside air. Another proposal would be to avoid dehumidifiers entirely by using solar distillation. Most areas where the Navy operates have available water sources which makes solar distillation a viable alternative for collecting distilled water for electrolysis.

In order to prove this system as mobile in the future, this entire production and storage facility can be scaled to the confines of a Conex style shipping container. With PV panels installed on the roof, dehumidifiers or distillation panels, the rest of the production and compression operation could be confined within. Utilizing a hydrogen microturbine or fuel cells, the system can store and produce power on demand at nearly any location. A system such as this could be moved relatively easy by sea or land to wherever a self-contained energy production facility is desired.

THIS PAGE INTENTIONALLY LEFT BLANK

APPENDIX A. SOLAR PANEL CONFIGURATION

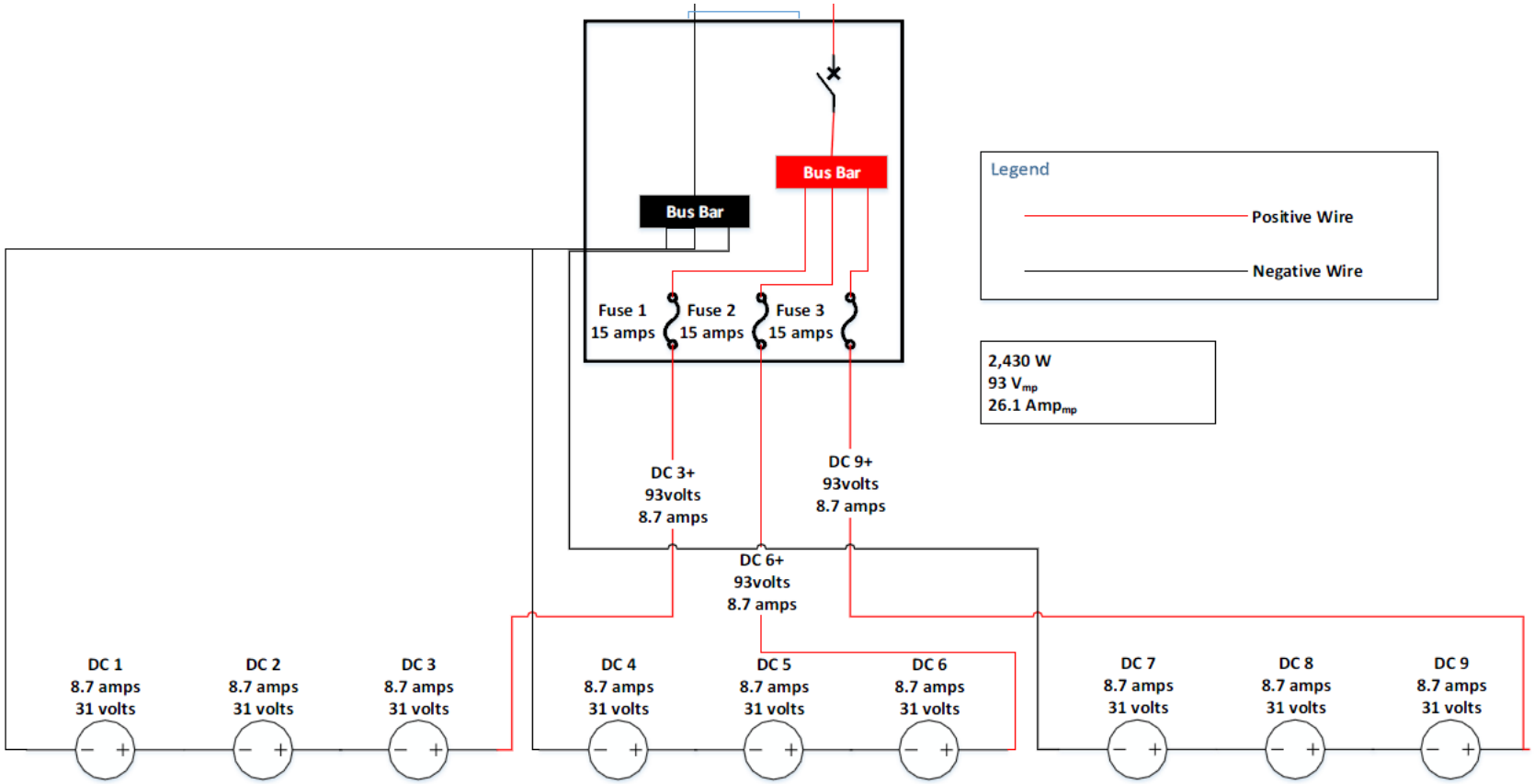

Figure 24. PV Array Diagram: Source [11].

THIS PAGE INTENTIONALLY LEFT BLANK

APPENDIX B. PRODUCTION CONFIGURATION

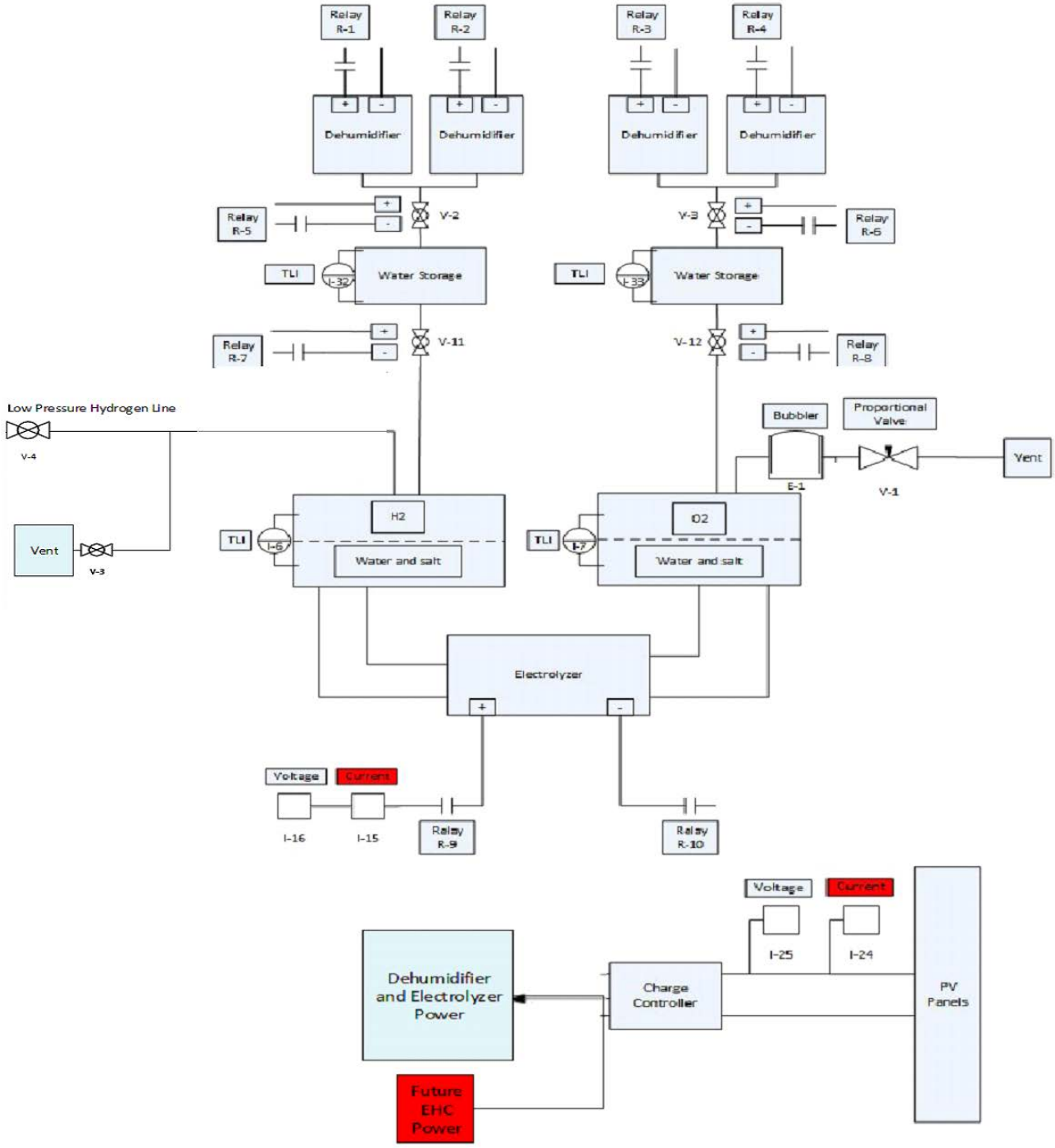

Figure 25. Production System Configuration. Adapted from [12].

THIS PAGE INTENTIONALLY LEFT BLANK

APPENDIX C. COMPRESSION AND STORAGE CONFIGURATION

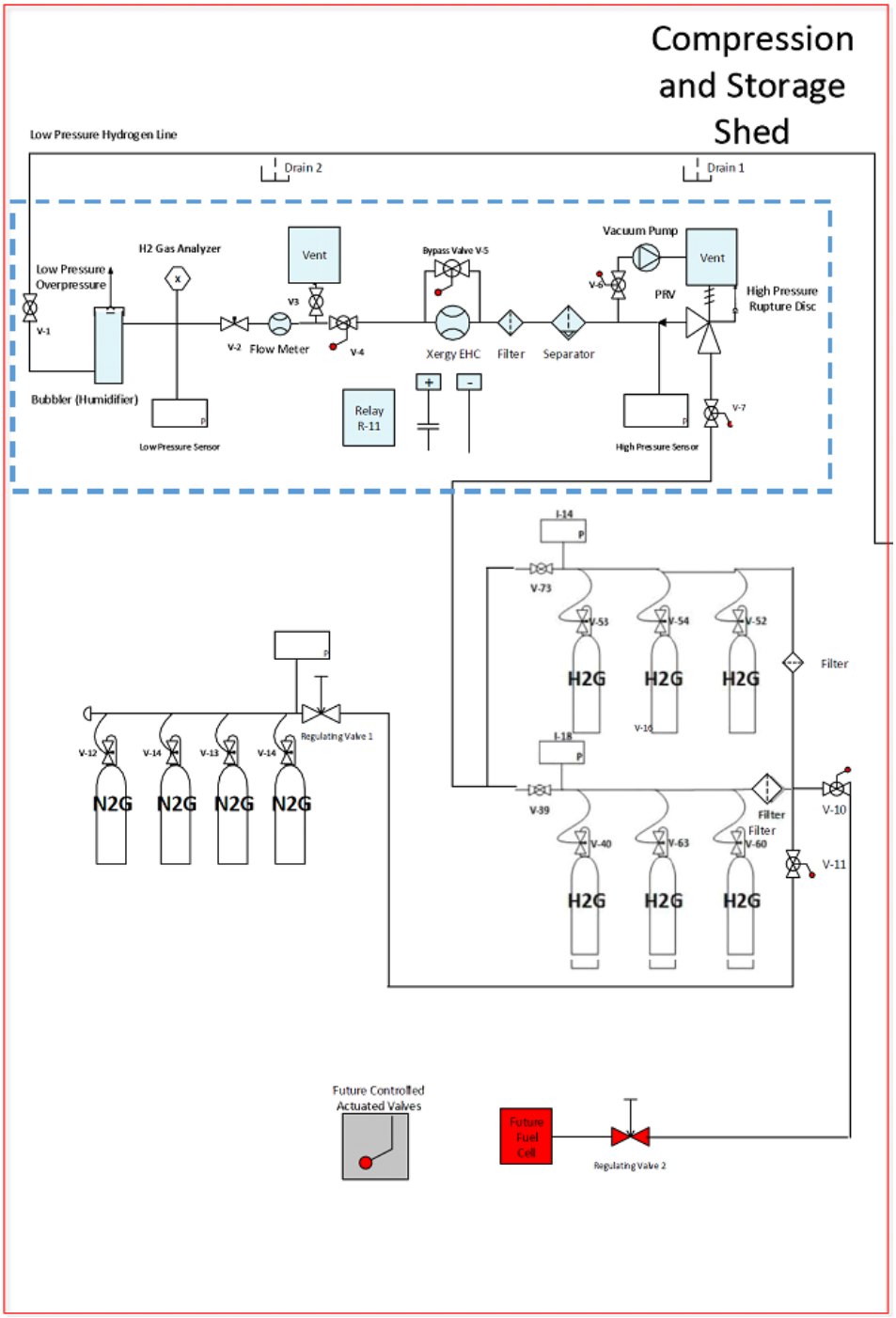

Figure 26. Compression and Storage Mechanical Diagram. Adapted from [13].

THIS PAGE INTENTIONALLY LEFT BLANK

APPENDIX D. ELECTRICAL WIRING CONFIGURATION

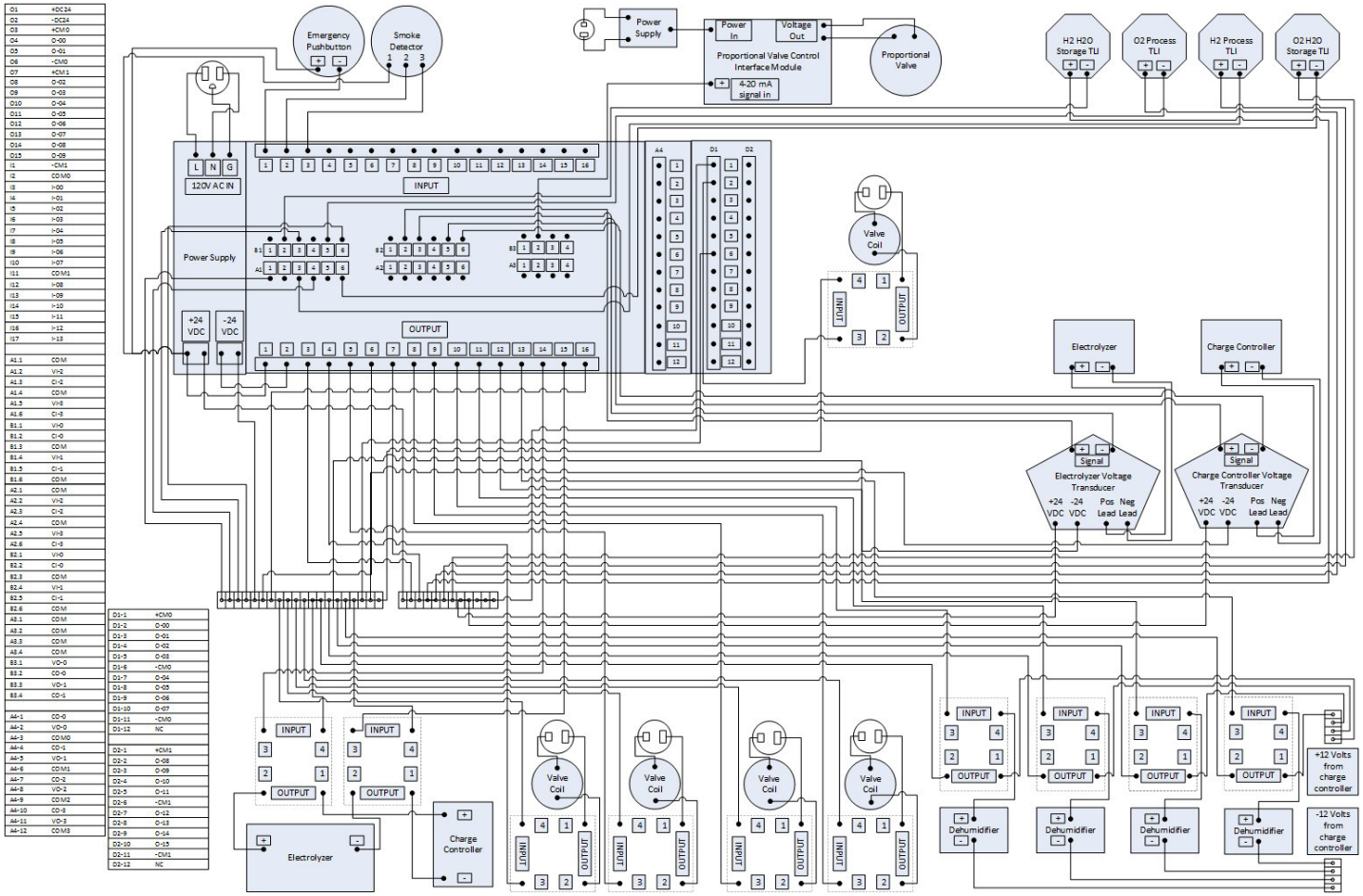

Figure 27. Electrical Diagram: Source [12]

THIS PAGE INTENTIONALLY LEFT BLANK

APPENDIX E. PLC CONNECTED COMPONENTS WORKBENCH CODE

Note: Using CCW, the code can be modified to change values within the variables section and script. PLC must be set to “Program” on the device and CCW must establish connection to device in order to make changes. PLC will run independent of connection to PC when set to “Run” on the device.
Further details on device operation and troubleshooting specific to the Allen Bradley Micro 850 PLC can be shown at the following link from the manufacturing company:
https://literature.rockwellautomation.com/idc/groups/literature/documents/um/2080-um002_-en-e.pdf

Controller.Micro850.Micro850.main

```
(*Get PV voltage*)
PV_Voltage:=mappingFunction(ANY_TO_REAL(_IO_P2_AI_01));

(*Check Solar Panels have at least 86V *)
IF PV_Voltage>=PV_min_Voltage THEN
        PVInput:=TRUE;
        TON_1(PVInput,TIME_DELAY_1);(*Start Timer*)
        IF TON_1.Q THEN
          ELECTROLYZER_ON_MASTER:=TRUE;
          turn_on_electrolyzer:=TRUE;
          PVInput:=FALSE;
          TON_1(PVInput,TIME_DELAY_1);(*Resetting and stopping timer*)
        END_IF;

END_IF;

(*Get water level for storage tanks*)
H2storageH2O:= tank_level_H2_Storage(ANY_TO_REAL(_IO_P1_AI_01));
O2storageH2O := tank_level_O2_Storage(ANY_TO_REAL(_IO_P1_AI_02));

IF H2storageH2O<storage_tank_min THEN
        start_dehumid_H2:=TRUE;
        storage_tank_low:=TRUE;
ELSIF O2storageH2O < storage_tank_min THEN
        start_dehumid_O2:=TRUE;
        storage_tank_low:=TRUE;
END_IF;

dehumid_H2_1_on:=TRUE;(*For testing*)
dehumid_H2_2_on:=TRUE;(*For testing*)
dehumid_O2_1_on:=TRUE;(*For testing*)
dehumid_O2_2_on:=TRUE;(*For testing*)

(*Turns on or off dehumidifiers based on fluid levels of storage tanks and voltage level on
electrolyzer*)
IF turn_on_electrolyzer AND NOT(dehumids_off) THEN
        IN_D:= TRUE;
```

```
        TON_D(IN_D, T#15s);

        _IO_EM_DO_07 := dehumidifiers_0(dehumid_O2_2_on, start_dehumid_O2, T#0s);
        _IO_EM_DO_06 := dehumidifiers_0(dehumid_O2_1_on, start_dehumid_O2, T#5s);
        _IO_EM_DO_05 := dehumidifiers_0(dehumid_H2_2_on, start_dehumid_H2, T#10s);
        _IO_EM_DO_04 := dehumidifiers_0(dehumid_H2_1_on, start_dehumid_H2, T#15s);

        IN_D:= FALSE;
        TON_D(IN_D, T#15s);

END_IF;

(*Get process level measurements*)
H2process_level := tank_level_H2_Pro(ANY_TO_REAL(_IO_P1_AI_00));(*Needs to get
calibrated for sensor*)
O2process_level := tank_level_O2_Pro(ANY_TO_REAL(_IO_P1_AI_03));(*Needs to get
calibrated for sensor*)

(*Checks to see if the process tank levels are too low. If they are then we want to fill them before
starting electrolyzer*)
IF (H2StorageH2O>lowest_storage_tank_level) AND
(O2StorageH2O>lowest_storage_tank_level) AND ((H2process_level + O2process_level)
<process_tank_sum_min) THEN
        fill_process_tanks := TRUE;
END_IF;

(*If there is enough voltage to turn on electolyzer AND the water storage tanks are NOT empty
ANT the fill process tanks are NOT full THEN turn on the electrolyzer pins*)
IF ELECTROLYZER_ON_MASTER AND NOT(storage_tank_low) AND NOT(fill_process_tanks)
THEN
        _IO_EM_DO_09 := TRUE;
        _IO_EM_DO_08 := TRUE;
END_IF;

(*Calculate electrolyzer voltage*)
electrolyzer_voltage:=mappingFunction(ANY_TO_REAL(_IO_P2_AI_00));

(*If the electrolyzer voltage is too low we start the pulse timer. the pulse timer runs until the time
elapses.
The dehumids off variable will turn off the dehumidifiers for 10 minutes, then turn them back on .*)
time_delay_2 := T#10M;
IF electrolyzer_voltage <= electrolyzer_min_voltage THEN
        ElectrolyzerInpout := TRUE;
        TP_1(ElectrolyzerInpout,time_delay_2);
        IF TP_1.ET <=  T#10M THEN
          dehumids_off :=TRUE;
          ElectrolyzerInpout := FALSE;
          TP_1(ElectrolyzerInpout,time_delay_2);
        END_IF;
END_IF;
```

APPENDIX F. MATLAB DATA COLLECTION CODE

Data Read Script
Benjamin Anderson
Ed Fosson

```
clear;clc;close all
```

Hydrogen Compression Station Data Acquisition Using NI CompactDAQ9184
(1) Verify COM port for Alicat Flow Meter using Device Manager (2) Open NI MAX and test CompacDAQ Chasis to verify communications (3) Enter filename below (4) Specify Runtime Establish Communications with Alicat Flow Meter using Troubleshooter
Filename and Runtime

```
delete(instrfindall) % Deletes the instruments currently connected
clear;clc;close all;
filename='514 test3' % filename
runtime =10*30; %Define iterations approx. 1 second
```

Establish NI DAQ connection

```
daqreset
devices = daq.getDevices
s = daq.createSession('ni')
```

Establish Alicat Flowmeter connection

```
flowMeter=serial('COM6','TimeOut',2,'BaudRate',19200,'Terminator','CR');
fopen(flowMeter);
```

Preallocate Data Arrays
type s.inputSingleScan in command bar to match size

```
timeint = zeros(1,runtime);
NIdata = zeros(9,runtime);
timerecord=zeros(1,runtime);
inletpressure=zeros(1,runtime);
inlettemp=zeros(1,runtime);
inletflow rate=zeros(1,runtime);
```

Pressure Transducer Calibration

```
Y1=500;     % 0-500psi 0.5-4.5V output
Y2=0;
X1=.5;
X2=4.5;
M1=500/4;
```

```
b1=-M1*.5;

Y3=3000;    % 0–3000psi 0.5-4.5V output
Y4=0;
M2=3000/4;
b2=-M2*.5;
```

NI Thermocouples Setup

```
addAnalogInputChannel(s,'1',0:1, 'Thermocouple');
tc1 = s.Channels(1);
set(tc1);
tc1.ThermocoupleType = 'K';
tc1.Units = 'Celsius';

tc2 = s.Channels(2);
set(tc2);
tc2.ThermocoupleType = 'K';
tc2.Units = 'Celsius';
% Option: Add cell thermocouple
```

Analog Channel Setup
Use Test Panels in NImax to configure correctly

```
addAnalogInputChannel(s,'3',0:3,'Voltage')
powersupply = s.Channels(1);
CurrentChargeController= s.Channels(2);
currenttransducer = s.Channels(3);
addAnalogInputChannel(s,'4',0:2,'Voltage');
previoustime=0; % initialize time counter
```

Loop for data collection

```
for i=1:runtime % # of samples to collect data for
 tic % starts a stopwatch
fprintf(flowMeter,'A');
IN=fscanf(flowMeter);
[OUT.ID,OUT.pressure,OUT.temp,OUT.LPM,OUT.SLPM,OUT.gas]=strread(IN,...
 '%s%f%f%f%f%s', 'delimiter', ' '); %reads flowmeter
inletpressure(i)=OUT.pressure; % psia
inlettemp(i)=OUT.temp; % Celcius
 NIdata(:,i) = s.inputSingleScan;
 inletflow rate(i)=OUT.SLPM; % SLPM
 timeint(i)=toc; % stops stopwatch to record data
 time(i)=previoustime+timeint(i); % adds time interval
 previoustime=time(i) % sets time for loop
 % option to add a pause if desired to reduce # of samples
end
```

Clean up the serial object

```
fclose(flowMeter);
delete(flowMeter);
clear flowMeter;
```

Data Reduction

```
T1=NIdata(1,:);                                 % Temperature (C)
T2=NIdata(2,:);                                 % Temperature (C)
Vstack=NIdata(3,:);                             % Voltage across stack
PVpower=NIdata(4,:)*50-40;                      % PV current
\
CompressorCurrent=(NIdata(5,:)+.0171)*5;        % Compressor Current (A)
CompPower=Vstack.*CompressorCurrent;
```

Write data to file

```
P1=(NIdata(7,:))*M1+b1;                           % Voltage to psia
P2=NIdata(8,:)*M2+b2;                           % Voltage to psia
P1=14.7+P1;                                     % psia to psig
P2=14.7+P2;                                     % psia to psig
CR=P2./P1;                                      % Compression Ratio
P1pa=P1*6894.76;                                % psi to kpa
P1pa=P1*6894.76;                                % psi to kpa
R=4124.5;                                       % Hydrogen gas constant
Tkel=T1+273;                                    % Kelvin
Tkel=T1+273;                                    % Kelvin
densityref=.08235/1000;                         % kg/m^3
mdot=inletflow rate./60*densityref;              % kg/s
wactual=CompPower/mdot/1000;                    % KJ/Kg
wisothermal=R.*Tkel.*log(CR);                   % KJ/Kg
gamma=1.4065;                                   % nondim
sigma=gamma./(gamma-1);                         % nondim
wadiabatic=sigma.*R.*Tkel.*[CR-1].^sigma;       %KJ/Kg
R=8.314;                                       % Universal Gas Constant
Tcell=((T1+T2)/2)+273.15;                       % Kelvin
n=50;                                         % number of cells (1 or 50)
F=9649;                                         % Farraday Constant
P1bar=P1*.0689;                                 % bar
P2bar=P2*.0689;                                 % bar
Vtheory=R.*Tcell./n./F.*log(CR);                % Volts
```

Write to File

```
A=[time',inletflow rate',P1',P2',T1',T2',Vstack',CompressorCurrent',...
    PVpower',CompPower',CR',inlettemp',inletpressure',wactual',wisothermal',...
    wadiabatic',Vtheory']; %17 Data Values
xlswrite(filename,A)
```

Plotting Data Collection

Rough Plots used onsite to assess runs

```
Figure(1)
plot(time, P2, time, P1)
title('Inlet/Outlet Pressure vs time')
xlabel('time (s)')
ylabel('Pressure (psi)')
legend('Exit Pressure','Inlet Pressure')

Figure(2)
plot(Vstack,CompressorCurrent)
title('Polarization Plot')
ylabel('Current (A)')
xlabel('Voltage (V)')

Figure(3)
plot(CompPower,inletflow rate)
title('CompPower,inletflow rate')
xlabel('Compressor Power (W) ')
ylabel('Flow Rate (SLPM)')

Figure(4)
plot(time,PVpower)
title('PV Power vs. Time')
xlabel('Time (s)')
ylabel('PV Power (W)')

Figure(5)
plot(CompressorCurrent,P2)
xlabel('Compressor Current (A)')
ylabel('Exit Pressure (psi)')

Figure(6)
plot(time,wactual,time,wadiabatic,time,wisothermal)
legend('w_(actual)','w_(adiabatic)','w(isothermal)')

Figure(7)
plot(P2,Vtheory,P2,Vstack);
xlabel('Pressure (bar)');
ylabel('Voltage (V)');
```

APPENDIX G. MATLAB POST-PROCESSING SCRIPT

Postprocessing Data Script
Ben Anderson

```
clear; clc; close all; % initialize workspace and closes opened Figures
DataImport=xlsread('514 test2.xls'); % reads file

smoother=100; % # surrounding data points for data smoothing
% 'sgolay' Savitzky-Golay FIR smoothing filter for noisy data
time=DataImport(:,1);                                    % sec
inletflow rate=DataImport(:,2);                           % SLPM
inletflow rate=smoothdata(inletflow rate);
P1=DataImport(:,3);                                      % psia
P2=DataImport(:,4);                                      % psia
P1=smoothdata(P1,'sgolay',smoother);
P2=smoothdata(P2,'sgolay',smoother);

T1=DataImport(:,5);                                      % C
T2=DataImport(:,6);                                      % C
T1=smoothdata(T1,'sgolay',smoother);
T2=smoothdata(T2,'sgolay',smoother);

Vstack=DataImport(:,7);                                  % V
Vstack=smoothdata(Vstack,'sgolay',smoother);

CompressorCurrent=DataImport(:,8);                       % V
CompressorCurrent=smoothdata(CompressorCurrent,'sgolay',smoother);

PVpower=DataImport(:,9);                                 % W
PVpower=smoothdata(PVpower,'sgolay',smoother);

inlettemp=DataImport(:,12);
inletpressure=DataImport(:,13);
```

Recalculated values

```
CR=P2./P1;                              % Compression Ratio
R=4124.5/1000;                          % Hydrogen Gas Constant
Tkel1=T1+273.15;                        % Kelvin
Tkel2=T2+273.15;                        % Kelvin
densityref=.08235;                      % kg/m^3
mdot=inletflow rate./60*densityref;      % kg/s
wactual=CompPower./mdot;                %KJ/kg
wisothermal=R.*Tkel1.*log(CR);          %KJ/kg
gamma=1.4065;
sigma=gamma/(gamma-1);

wadiabatic=sigma*R.*Tkel1.*((P2./P1).^((gamma-1)/(gamma))-1); %KJ/kg
```

```
Rbar=8.314;                              % ideal gas constant
Tcell=((T1+T2)/2)+273.15;                % Kelvin (approximated value)
cells=1;                                 % 1 or 50
n=2;                                     % reaction number
F=9649;                                  % Faraday Constant
P1bar=P1*.0689;                          % bar
P2bar=P2*.0689;                          % bar
Vtheory=Rbar.*Tcell./n./F.*log(CR);      % V
```

Plotting Data

```
Figure(1)
yyaxis left
plot(time, P2*.06894757, time, P1*.06894757)
title('Inlet/Outlet Pressure and Flow rate vs time')
xlabel('time (s)')
ylabel('Pressure (bar)')

yyaxis right
plot(time, inletflow rate,'r')
ylabel('Flow Rate (SLPM)')
legend('Exit Pressure','Inlet Pressure','Flow Rate','location','east')
```

```
Figure(2)
plot(Vstack*3,inletflow rate)
title('Flow Rate vs Compressor Voltage')
ylabel('Flow Rate (SLPM)')
xlabel('Voltage (V)')
```

```
Figure(3)
plot(CompPower,inletflow rate)
title('CompPower,inletflow rate')
xlabel('Compressor Power (W) ')
ylabel('Flow Rate (SLPM)')

Figure(4)
plot(time,PVpower)
title('PV Power vs. Time')
xlabel('Time (s)')
ylabel('PV Power (W)')

Figure(5)
plot(CompressorCurrent,P2)
xlabel('Compressor Current (A)')
ylabel('Exit Pressure (psi)')
```

```
Figure(6)
yyaxis left
plot(P2bar,wisothermal./wactual*100,P2bar,wadiabatic./wactual*100)
xlabel('Outlet Pressure (bar)')
ylabel('Adiabatic and Isothermal Efficiency (%)')
title('Efficiency vs Outlet Pressure')
```

```
yyaxis right
plot(P2bar,Vtheory*cells.*100/Vstack)
ylabel('Nernst Efficiency (%)')

legend('isothermal efficiency','adiabatic efficiency','Nernst
efficiency','location','south')
```

THIS PAGE INTENTIONALLY LEFT BLANK

LIST OF REFERENCES

[1] U.S. Energy Information Administration, "Defense Department energy use falls to lowest level since at least 1975," February 5, 2015. [Online]. Available: https://www.eia.gov/todayinenergy/detail.php?id=19871

[2] Department of the Navy, "Strategy for renewable energy." October 2012. [Online]. Available: https://www.secnav.navy.mil/eie/Documents/DoNStrategyforRenewableEnergy.pdf

[3] J. Powers, "The military is leading the march toward energy independence," Green Tech Media, 20 July 2017. [Online]. Available: https://www.greentechmedia.com/articles/read/the-military-is-leading-the-march-toward-energy-independence#gs.4imq2s

[4] Energy Efficiency and Renewable Energy, "Hydrogen production." Accessed December 12, 2018. [Online]. Available: https://www.energy.gov/eere/fuelcells/hydrogen-production

[5] I. Dincer, "Green methods for hydrogen production," *International Journal of Hydrogen Energy*, vol. 37, no. 2, Jan. 2012, pp. 1954–71. [Online]. https://doi.org/10.1016/j.ijhydene.2011.03.173.

[6] Energy Efficiency and Renewable Energy, "Hydrogen Production." U.S. Department of Energy, January 2007. [Online]. Available: https://www.energy.gov/eere/fuelcells/hydrogen-production

[7] G. Crabtree, M. Dresselhaus, and M. Buchanan, "The Hydrogen Economy," IEEE Engineering Management Review, vol. 34, no. 4, pp. 7–16, Jan. 2007. [Online]. https://doi.org/10.1109/EMR.2006.261397

[8] J. Penley, "Gas Turbine Operation on Compressed Hydrogen," M.S. thesis, Mech. Egr. Dept., Naval Postgraduate School, Monterey, CA, USA, 2018. [Online]. Available: https://calhoun.nps.edu/handle/10945/61244

[9] K. Bennaceur, B. Clark, O. Franklin, T. Ramakrishnan, C. Roulet, and E. Stout. "Hydrogen: A future energy carrier?" *Gas 25*, no. 20, pp. 30–41, spring 2005. [Online]. Available: https://www.slb.com/~/media/Files/resources/oilfield_review/ors05/spr05/03_hydrogen_a_future_energy.pdf

[10] A. Aviles, "Renewable production of water, hydrogen, and power from ambient moisture," M.S. thesis, Mech. Egr. Dept., Naval Postgraduate School, Monterey, CA, USA, 2016. [Online]. Available: https://calhoun.nps.edu/handle/10945/51584

[11] S. F. Yu, “Analysis of an improved solar-powered hydrogen generation system for sustained renewable energy production,” M.S. thesis, Mech. Egr. Dept., Naval Postgraduate School, Monterey, CA, USA, 2017. [Online]. Available: https://calhoun.nps.edu/handle/10945/56854

[12] S. M. Birkemeier, “Industrial Automation of solar-powered hydrogen generation plant,” M.S. Thesis, Mech. Egr. Dept., Naval Postgraduate School, Monterey, CA, USA, 2018. [Online]. Available: https://calhoun.nps.edu/handle/10945/59700

[13] E. A. Fosson, “Design and analysis of a hydrogen compression and storage station,” M.S. thesis, Mech. Egr. Dept., Naval Postgraduate School, Monterey, CA, USA 2017. [Online]. Available: https://calhoun.nps.edu/handle/10945/56919

[14] National Hydrogen Association, U.S. DOE, “The history of hydrogen,” Jul. 14, 2010, p. 1. [Online]. Available: https://web.archive.org/web/20100714141058/http:/www.hydrogenassociation.org/general/factSheet_history.pdf

[15] A. Sarkar and R. Banerjee, “Net energy analysis of hydrogen storage options,” *International Journal of Hydrogen Energy*, vol. 6, no. 8, pp. 867–877, Jul. 2005. [Online]. Available: https://doi.org/10.1016/j.ijhydene.2004.10.021.

[16] N. Stetson, “Hydrogen storage program overview,” U.S. Department of Energy, October 2013. [Online]. Available: https://www.hydrogen.energy.gov/pdfs/progress13/iv_0_stetson_2013.pdf

[17] National Renewable Energy Laboratory (NREL), “Hydrogen compressor reliability investigation and improvement,” Cooperative Research and Development Final Report CRD-13-514, March 2016. [Online]. Available: https://www.nrel.gov/docs/fy16osti/66027.pdf

[18] L. Lipp, “Electrochemical hydrogen compressor.” Final Scientific/Technical Report Under DOE Award Number DE-EE003727, Fuel Cell Energy Inc., May 17, 2012. [Online]. Available: https://www.hydrogen.energy.gov/pdfs/review12/pd048_lipp_2012_o.pdf

[19] World Weather and Climate Information, “Monterey, California-Humidity.” Accessed May 21, 2019. [Online]. Available: https://weather-and-climate.com/average-monthly-Humidity-perc,monterey-california-us,United-States-of-America

[20] H. Kim, S. R. Rao, E. A. Kapustin, L. Zhao, S. Yang, O. M. Yaghi, and E. N. Wang, “Adsorption-based atmospheric water harvesting device for arid climates,” *Nature Communications*, Mar. 22, 2018. [Online]. Available: http://yaghi.berkeley.edu/pdfPublications/NComm2018.pdf

[21] Energy Sage, “What are the most efficient solar panels on the market? Solar Efficiency Explained,” March 1, 2019. [Online]. Available: https://news.energysage.com/what-are-the-most-efficient-solar-panels-on-the-market/

[22] I. Penn, “California invested heavily in solar power. Now there’s so much that other states are sometimes paid to take it,” *LA Times*, June 22, 2017. [Online]. Available: https://www.latimes.com/projects/la-fi-electricity-solar/

[23] C. Thomas, “Fuel cell and battery electric vehicles compared,” *International Journal of Hydrogen Energy*, vol. 34, no. 15, pp. 6005–6020, 2009. https://doi.org/10.1016/j.ijhydene.2009.06.003

[24] M. Dansie, “Supercapacitors vs Lithium-ion,” Revolution Green, February 19, 2015. [Online]. Available: https://revolution-green.com/supercapacitors-vs-lithium-ion/

[25] O. Ulleberg, T. Nakken, and A. Eté, “The wind/hydrogen demonstration system at Utsira in Norway: Evaluation of system performance using operational data and updated hydrogen energy system modeling tools,” *International Journal of Hydrogen Energy*, vol. 35 no. 5, pp. 1841–1852, 2010. [Online]. Available: https://doi.org/10.1016/j.ijhydene.2009.10.077

[26] M. Ball and M. Weeda, “The Hydrogen Economy – Vision or Reality?” *International Journal of Hydrogen Energy*, vol. 40, no. 25, pp. 7903–7919, Jul. 6, 2015. [Online]. https://doi.org/10.1016/j.ijhydene.2015.04.032

[27] G. Ka’iliwai and R. Roley, “PACOM energy initiatives,” U.S. Pacific Command, May 2010. [Online]. Available: http://e2s2.ndia.org/pastmeetings/2010/tracks/Documents/9959.pdf

[28] Fortune, “GM is working with the U.S. Navy to bring hydrogen power to underwater drones,” June 23, 2016. [Online]. Available: http://fortune.com/2016/06/23/gm-navy-hydrogen-fuel/

[29] Business Wire, “U.S. Naval Research Lab selects Alta Devices to add solar Power to its breakthrough Hybrid Tiger UAV Project.” May 14, 2018. [Online]. Available: https://www.businesswire.com/news/home/20180514005480/en

[30] Compressed Gas Association Inc.,*CGA G-5-2017 Hydrogen*, Chantilly, VA, USA, 2017, pp. 1–8.

[31] National Fire Protection Association,*NFPA 2 Hydrogen Technologies Code 2016 Edition*, Quincy, MA, USA, 2016, pp. 2–45.

[32] Compressed Gas Association Inc.,*CGA G-5.4-2012 Standard for Hydrogen Piping Systems at User Locations* Chantilly, VA, USA, 2012, pp.7.

[33] American Society of Mechanical Engineers, *ASME B31.12 Hydrogen Piping and Pipelines*, New York, NY, USA, ch. 5, sec. 5 Tubing Joints, p. 95.

[34] American Institute of Chemical Engineers, Center for Chemical Process Safety, *Inherently Safer Chemical Processes: A Life Cycle Approach*, New York, NY, USA: John Wiley and Sons, Inc., 2013, p. 9.

[35] D. Crowl, *Understanding Explosions*, Center for Chemical Process Safety, New York, NY, USA: John Wiley and Sons, Inc., 2003, pp. 122–125.

[36] M. Early, C. Coache, M. Cloutier, G. Moniz, and D. Vigstol, *National Electrical Code Handbook*, 14th ed., National Fire Protection Association, Quincy, MA, USA, 2016, p.587.

[37] Parker, "High Pressure Filters." Accessed December 1, 2018. [Online]. Available: https://www.parker.com/Literature/IGFG/PDF-Files/HighPressure.pdf

INITIAL DISTRIBUTION LIST

1. Defense Technical Information Center
   Ft. Belvoir, Virginia

2. Dudley Knox Library
   Naval Postgraduate School
   Monterey, California